Worcester Polytechnic Institute
Digital WPI

Major Qualifying Projects (All Years)

Major Qualifying Projects

May 2014

Dual Assay Study of Antisense Transcript Regulation of Meiotic Genes during Mitotic Growth in Schizosaccharomyces pombe

Ryan William Holmes
Worcester Polytechnic Institute

Follow this and additional works at: https://digitalcommons.wpi.edu/mqp-all

Dual Assay Study of Antisense Transcript Regulation of Meiotic Genes during Mitotic Growth in *Schizosaccharomyces pombe*

A Major Qualifying Project Report

Submitted to the Faculty of the

WORCESTER POLYTECHNIC INSTITUTE

In partial fulfillment of the requirements for the

Degree of Bachelor of Science in Chemistry

By

_____

Ryan Holmes

Date: May 1, 2014

Approved:

<table>
<tr><td>_____</td><td>_____</td></tr>
<tr><td>Nicholas Rhind. Ph.D.
Department of Biochemistry
    and Molecular Pharmacology
UMass Medical School
Major Advisor</td><td>Destin Hielman Ph.D.
Department of Chemistry
    and Biochemistry
WPI Project Advisor</td></tr>
</table>

TABLE OF CONTENTS

Acknowledgements

I would like to begin by thanking Dr. Nicholas Rhind at the University of Massachusetts Medical School for giving me the opportunity to work in his lab. His patience and support was what made the project possible. In addition I would like to thank, Livio Dukaj for his continuous help and direction on everything from protocol to proper technique. I wish to thank the rest of the Rhind Lab for their guidance and willingness to teach me whenever needed. I also wish to thank Dr. Destin Heilman for his aide on the thesis and presentation aspects of the project.

Abstract

Gene regulation is an integral part of cellular function and key to understanding how genetic material is expressed in prokaryotes and eukaryotes. One of the regulatory pathways is hypothesized to be the interaction of sense and antisense transcripts that lead to the degradation of the dsRNA and consequently transcriptional regulation. The Rhind Lab has shown that certain meiotic genes in *S. pombe* have statistically high antisense transcripts that would be needed for this type of regulation. The sense and antisense mediated RNA regulation model was investigated by direct transcript analysis by qRT-PCR without the presence of any double-strand specific ribonucleases. The transcriptional analysis suggested a more biologically complex interaction. Another method utilized a RFP/GFP reporter that changed expression of one fluorescent protein for the other in vivo. The development of this assay is under construction and is needed for the confirmation that the sense and antisense transcription is part of gene regulation. The in vivo assay accompanied by the qRT-PCR data could suggest a specific case where antisense transcription plays a biological role in gene regulation adding to the complexity of the RNAi pathway.

Table of Figures

Table of Tables

1.0 Introduction

1.1   *Schizosaccharomyces pombe* **as a model organism**

    S. pombe is a unicellular archiascomycete fungus that is part of a unique branch fungi that are used as model organisms for genetic and biochemical research. Although *S. pombe* which is part of the fission yeast classification, is unicellular it also participates in many of the same biological functions as high eukaryotes. (26) The species diverged from its close relative *Saccharomyces cerevisiae*, a fission yeast, an estimated 330-420 million years ago and similarly diverged from metazoans and plants an estimated 1,000 -1,200 million years ago. (35) *S. pombe* has proven to be a useful organism in the scientific field since its discovery.

    S. pombe was first introduced to geneticists in the 1890s and was extensively examined during the course of the 1950s leading up to its genome sequencing in 2002. A DAP1 stained image of vegetatively growing *S. pombe c*ells is depicted in Figure 1. Once *S. pombe* joined the ranks as the sixth model eukaryote organism to have its genome sequenced its true potential was elucidated. (36) *S. pombe* was found to be a significant organism as it had the smallest number of predicted genes than any other recorded eukaryote. Even when compared to *S. cerevisiae, S. pombe* still had just under 1000 less predicted genes. (26) The small number of genes coupled with the *S. pombe* genome size, 13.8-Mbp comprised of three chromosomes, made the study of cell-cycle control, mitosis and meiosis,
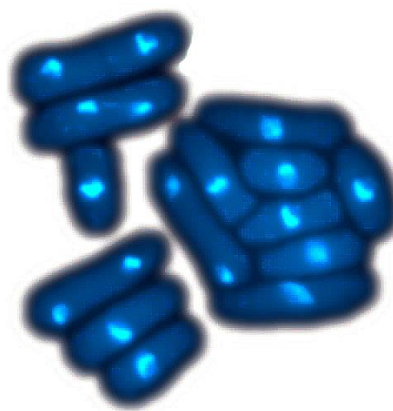
Figure 1: Mitotic growth in the fission yeast *S. pombe*

An image of Mitotic growth in the fission yeast *S. pombe* that has been stained with DAP1 to highlight the nucleus. The nuclear changes that take place during the mitotic life cycle are clearly shown.

DNA repair and recombination, and checkpoint controls easier for geneticist to explore. (35)

A small genome, a limited number of genes, and an organism that can be genetically manipulated with ease sets the stage for scientific exploration in a number of cellular functions. (35) Exploration into these areas such as DNA replication, RNA transcription, and gene expression are a few examples of what this simple eukaryote can give insight into. This research could be analogous to far more complex systems and pathways present in the higher eukaryotes.
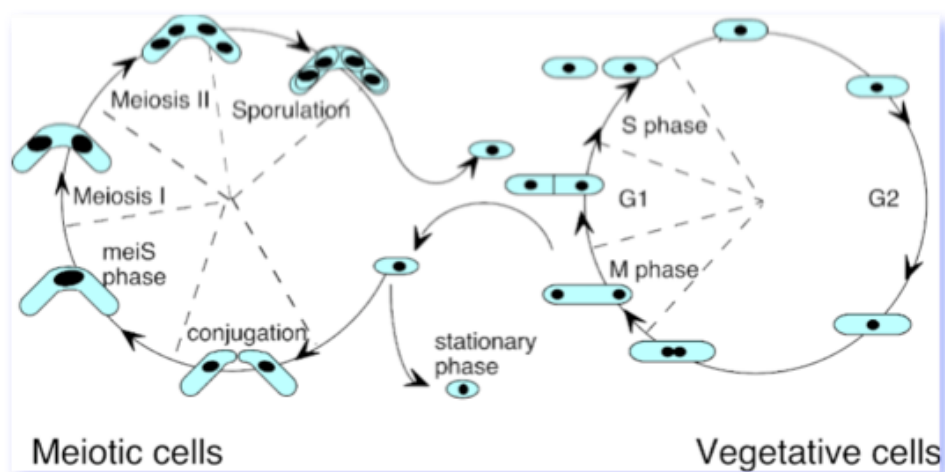
Figure 2: Two Life Cycles of Fission Yeast

This image shows vegetative or mitotic growth on the right and the meiotic
cycle on the left illustrating the general life cycle of fission yeast.

1.2 *S. pombe* **Life Cycle**

S. pombe is part of the fission yeast clade and follows both a mitotic and meiotic growth cycle as shown above in Figure 2. The type of mitotic division is classified by the fission yeast clade where the yeast cells divide by medial fission. (9) During G2 the cells elongate from the poles of the cylindrical cell in preparation for division. (14) The elongation of the yeast cells can be measure and used as an indicator of the cell's mitotic progression. (14) Once the cells are committed to mitosis, elongation stops and the cells progress though M phase and then G1. The

formation of the septum at the geometric middle of the cell sets the stage for cytokinesis and the resulting division producing two daughter cells of equal size. (8) The daughter cells then elongate and proceed to enter the mitotic cycle again by initiation into G2.

The alternate cell cycle as presented on the left side of Figure 2 represents the meiotic cell cycle where the yeast undergoes sexual differentiation. In the absence of sufficient nutrients, the opposite mating types h^- and h^+, *S. pombe* cells will commence conjugation. (28) The newly conjugated cells form a diploid zygote which enter meiosis and consequently sporulation. The tetrad ascus formed contains the new haploid spores. The spores will remain until permissive conditions return allowing the spores to fuse, enter G2, and commence elongation.

1.3 RNA Transcription

RNA transcription is an integral part of all life and is an important area of biological study that is used to gain insight into many essential pathways for gene expression, protein synthesis, and many other significant biological functions. RNA transcription can be separated into three distinct stages namely initiation, elongation, and termination. The first stage of RNA transcription, initiation begins when the Preinitation Complex (PIC) is formed by binding the RNA polymerase complex. The promoter of the gene contains a consensus sequence upstream of the transcription start site that is recognized by the general transcription factors (GFTs). The GFTs bind to the double stranded DNA and recruit the RNA Polymerase II core. The PIC once bound to the DNA will begin the process of copying the DNA.

The process of synthesizing the RNA transcript from the DNA sequence is called elongation. The PIC will generate a transcription bubble and move downstream from the transcription start site in the 5' to 3' direction. This will result in the synthesis of the nasant RNA transcript that is cotranscriptionally processed by the carboxyl tail doman (CTD) on the

PIC as it is being extruded. The CTD is responsible for the processing of the 5' and 3' ends of

the RNA transcript by the addition of a 7-methylguanosine triphosphate cap and a poly(A) tail,

which serve to protect the transcript from degradation once it leaves the nucleus. The RNA

transcripts are processed further by post transcriptional splicing mechanism. Once RNA

processing is completed the resultant mature RNA product that will then leave the nucleus to be
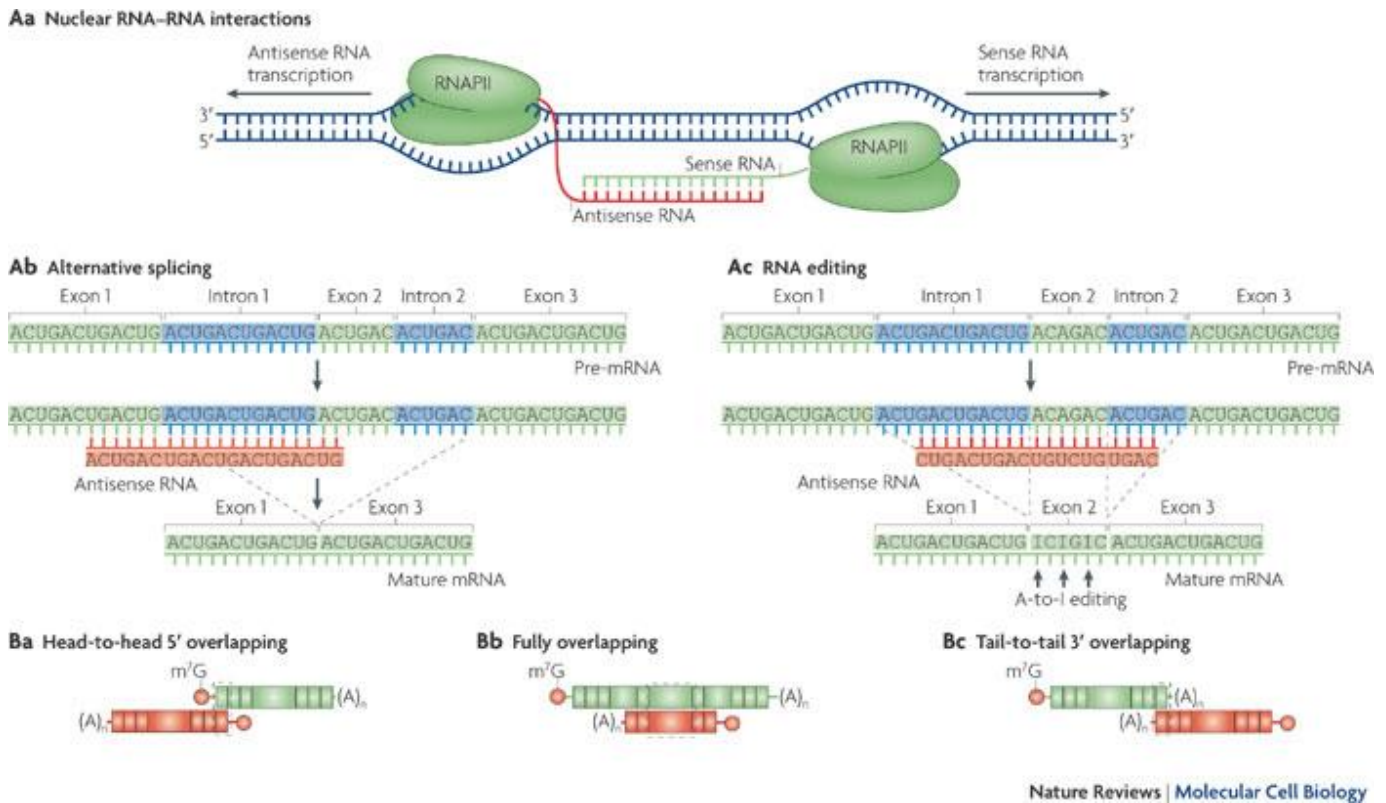
Figure 3: RNA Duplex Formation

This is image depicts both sense and antisense transcription with some proposed consequences
of nuclear RNA duplex formation.

translated in the cytosol by the ribozyme.

Before the GFTs can attract the PIC, the GTFs must bind to the either the Watson or the

Crick DNA strand associated with a gene before initiation can commence. When a gene is

transcribed in the normal direction from either the Watson or Crick strand it is referred to as a

sense transcript. When the opposite strand of complementary sequence is transcribed for the

same gene it is called the antisense transcript. The sense and antisense transcripts comprise two oppositely orientated RNA molecules with perfect double strand homology as displayed in Figure 3, but only one codes for a functional protein. (27) The homology between the two strands has been shown to create double strand RNA duplexes. (2) The pathway for the formation of RNA double stranded duplexes has been theorized and is represent in the figure above.

Evidence shows that many organisms, including higher eukaryotes, make antisense transcripts as a byproduct bidirectional transcription. (11) With this mind there are two types of duplex RNAs that can be formed from the complementary sequences of RNA. There are both short or imperfect and long or perfect double strand RNA duplexes that can form. The short duplexes are RNA transcripts that are no larger than one hundred base pairs and are most likely produced from transcriptional activity at different loci. The opposite long RNA duplexes are most likely formed by opposing transcription at the same locus. These two types of RNA duplexes are postulated to form both in the nucleus and the cytosol and serve as mechanism for gene regulation possibly at the transcriptional level. (2, 11)

The way that the short and long RNA duplexes are formed is theorized and illustrated in Figure 3. The figure is split into the two theories of where the RNA duplex is formed either in the nucleus or the cytosol. The image Aa on the top of Figure 3 shows the nuclear interpretation for RNA duplex formation where the oppositely transcribed RNA form a duplex contranscriptionally or post transcriptionally in the nucleus. This could lead to either alternative splicing or the complications in RNA editing (Fig. 3 Ab and Ac) due to the RNA duplex interference in identification of introns. (2) The other hypothesis where the RNA duplex forms outside of the nucleus has the ability to inhibit translation and reduce transcript stability. Figure

3 Ba – Bc proposes three different cytosolic binding motifs that would result in RNA duplex formation. The RNA duplex could aid in the generation of RNA hairpins or mask RNA binding sites. RNA duplexes formed within the cytosol are likely to inhibit translation by delaying association with the ribozyme and consequently slowing protein synthesis. (2)

Both the nuclear and cytosolic hypotheses support that the production of RNA duplexes from the sense and antisense transcripts could result in endo- or exonuclease degradation of the RNA transcripts via RNases. (2, 11, 27) The RNA duplex could affect transcript stability by initiating the RNAi pathway where by the double stranded RNA duplex is recognized as exogenous nucleic acids and is degraded into siRNAs.

1.4   RNAi Pathway

The RNAi pathway is biologically conserved mechanism used in response to the detection of either endogenous or exogenous double stranded RNA. The RNAi pathway is used as a means for the cell to protect itself and for gene regulation by the production of miRNAs or siRNAs. In the formation of both miRNAs and siRNAs, is performed by the biological machine called Dicer (Dcr1) which is used to identify double stranded RNA. The RNA duplex formed by the sense and antisense transcripts is detected by the Dcr1 machine and bound to it. Once bound Dcr1 cuts the double stranded RNA into approximately twenty-two nucleotide long pieces that are then bound to another complex, RISC (RNA-induced silencing complex). The RISC complex unwinds the short double stranded RNA molecules and separates the two strands into single stranded RNA. The resulting short single stranded RNA becomes miRNA or siRNA that the RISC complex can use to repress the translation or degrade mRNA transcripts that are transcribed later. The differentiation between siRNAs and miRNAs is the function that they are

associated with. miRNAs are used as means of silencing translation while siRNAs are used to

degrade mRNA.
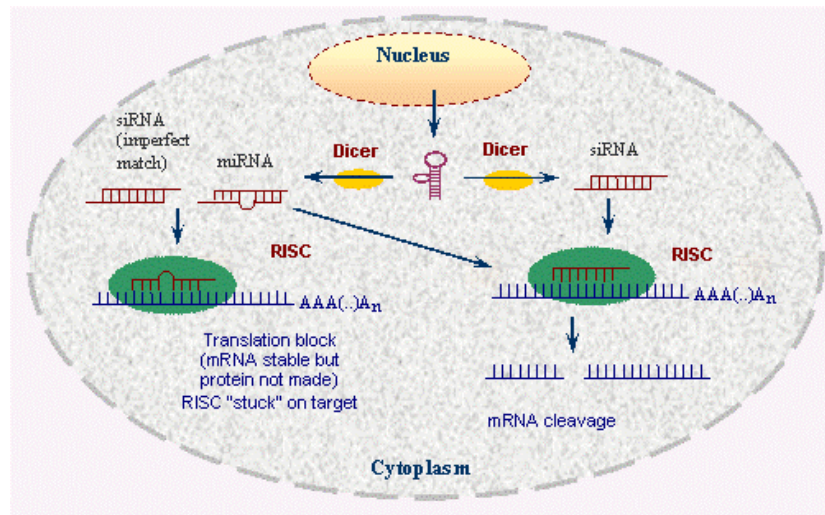
Figure 4: Ribonuclease involvement in RNAi

A model for the RNAi pathway utilizing ribonuclease enzymes to illustrate the how dsRNA is
degraded into miRNA or siRNA.

S. pombe employs two double strand ribonucleases, Dcr1 and Pac1 in its RNAi pathway.

Both enzymes have the ability to degrade the double stranded RNA of the sense, antisense

transcript duplex. (4, 24) Dcr1 has been shown to function with ago1 and rpd1 in the RNAi

pathway. There is also evidence to suggest that these three genes are involved in the formation

and maintenance of heterochromatin and chromosome segregation. (4) Dcr1 is active in gene

silencing and has implications as a post transcriptional regulator. (7)

Unlike Dcr1, Pac1 is an essential gene for mitotic growth that is associated with the

synthesis of ribosomal RNA precursors. (10) Pac1 functions not only as a double stranded

RNase belonging to the RNase III class but also as a mutlicopy suppressor for pat1 which helps

direct entrance into meiosis. The overexpression of the gene suppresses the cells entrance into

meiosis by inhibiting the pat1 as well as prevents all sexual differentiation. (23)

1.5   Bidirectional Transcription *S. pombe*

There is emerging evidence that shows RNA transcription takes place on both DNA strands for a given gene. *S. pombe* is no exception as almost one third of its protein coding DNA regions contain elevated levels of antisense transcription. (19) The abundance of antisense transcripts found in the yeast genome suggests new functions of noncoding RNAs (6) could lead to a pathway for gene regulation and silencing that could take place at the transcriptional level. (3) The finding of transcription at significant levels adds another layer of complexity to the *S. pombe* transcriptome and sets the stage for the study of new functions of ncRNAs.

Of these bidirectionally transcribed genes there is significant evidence showing that the majority belong to the meiotic and stress response genes. (5, 19, 22) The relative abundance of the antisense transcript has been determined to be higher than that of its sense counterpart in one hundred sixteen genes, where the resulting RNAs correspond to mid-meiotic genes. (5) This phenomena is observed by the deep sequencing plot for Spo6 in Figure 5. This expression of these antisense transcripts is seen in mitotic growing cells where little or no mRNA is expected, could suggest that antisense transcripts can act as regulators.
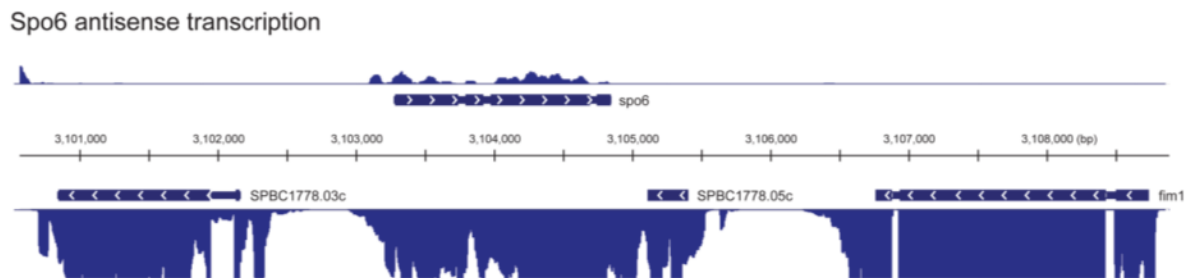
Figure 5: High Antisense Transcription is Present at Specific Meiotic Genes

The plot shows transcription on the Watson and Crick DNA strands on the top and bottom, respectively. The reads from RNA-Deep Sequencing experiments are displayed on a scale of 0—300 and plotted against the chromosomal coordinates. Signals greater than 300 were truncated so that all low amplitude signal could be seen. The gene of interest, meiotic gene Spo6, shows significantly higher antisense transcription than the corresponding sense transcription.

The mitotic and meiotic cell cycle shown in Figure 2 is paralleled with a stark change in transcription in the yeast cells. During mitotic growth there must be a tightly controlled elimination of any mRNA of meiosis specific transcripts to ensure that the cells do not enter into an undesired meiosis. (1) This has been shown using DNA microarrays to watch meiotic expression of these genes. The data collected showed regulated waves of transcription that allowed for many biological functions necessary for a successful meiotic cycle. (13) The regulation of these genes is important to the function of the yeast cells during mitotic growth and antisense transcription could one of the many ways in which these genes are regulated.

Two of examples of the mid-meiotic genes that produced higher antisense transcription than sense transcription are the *S. pombe* genes Spo6 and Spo4. Spo6 has been identified as gene related to sporulation, required for the initiation of DNA replication and regulated by Mie4 as a forkhead transcription factor. (17) During the study of Spo6 function it was determined that the antisense transcription level is high relative to the sense transcription during vegetative growth. Spo6 transcription changes with the onset of meiosis. (22) The arrival of the new cell cycle allows the sense transcript to proliferate and the antisense to diminish. (17) The function of spo6 in DNA initiation has been investigated because the Spo6 gene codes for a protein of similar sequence to budding yeast *S. cerevisiae*'s Dbf4p which is a regulatory protein subunit of Cdc7p protein kinase complex. Dbf4p associates with Cdc7p and binds to the DNA PIC to start initiation by phosphorylating MCM proteins permitting DNA replication. (17)

Spo4 similar to Spo6 is also a meiotic induced gene that is involved in sporulation during Meiosis II. The Spo4 associates with its regulator Spo6 by the formation of an active kinase complex. Spo4 unlike Spo6 is not essential for mitosis or DNA replication, but is required proper progression through Meiosis II. (18) The function of Spo4 is exposed when looking at the

preferential nuclear localization of the protein without Spo6 requirement. This suggests that Spo4 is a Cdc7 kinase (18) and more specifically a serine, threonine protein kinase.

1.6   Reporter Cassettes

Any time that transcription is analyzed and assayed for, a method must be employed to distinguish when the transcript is produced or not. A common method used for *in vivo* research in transcript analysis is the employment of Green Fluorescent Protein (GFP) and Red Fluorescent Protein (RFP) as a reporter cassette. For example GFP or RFP cassettes could be inserted into the yeast genome such that when the RNA transcript of interest is transcribed, one of the fluorescent proteins is also transcribed. When the RNA transcript is not present no fluorescent protein in produced. Under fluorescent light the yeast can be analyzed and the amount of fluorescent protein quantized.

GFP or 1EMP was isolated from the bioluminescent jellyfish *Aequorea victoria* found in the north Pacific. (15) The jellyfish use aequorin, a bioluminescent protein to emit blue light that the 1EMP absorbs and consequently emits green light. (29)

The GFP is comprised of 230 residues where the protein shown in Figure 6. The shape of the protein tertiary and quaternary structure is described as a beta-

Figure 6. Structure of 1EMP beta-can.

can where the protein consists of a "cylinder comprising of eleven strands of beta-sheet with an alpha-helix inside and short helical segments on the ends of the cylinder." (29, 37) RFP is a homologue to GFP isolated from reef coral and anemone that emits red spectral light. RFP subunits adopt similar shape to that of GFP beta-can confirmation. (33)
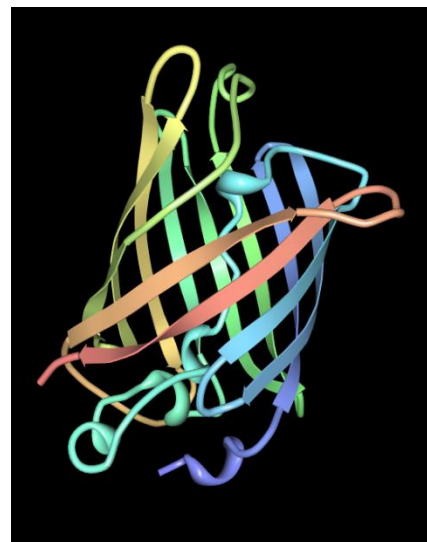
Both GFP and RFP are part of the fluorescent protein family that spontaneously fluoresce by autocatalytic chromophore generation. (15) The chromophores of the fluorescent proteins are comprised of an internal tripeptide that is protected inside of the cylinder of the structure. (37) In the case of GFP the tripeptide is Ser65-Tyr66-Gly66 where the three subsequent amino acids catalyze the reactions with 4-(p-hydroxybenzylidene)-5-imidazolinone. The local chemistry and chemical groups near the chromophore determine the wavelengths of light both absorbed and emitted. (15) The short amino acid sequence of the fluorescent proteins and the local chemistry of the chromophore makes the proteins easily manipulated for a variety of biological functions. (15)

Another reporter cassette that is often employed is the Cre-loxP System. Cre-loxP is an example of a site specific recombinase that is comprised of Cre complex and the sequence of DNA that the Cre complex binds which is referred to as a loxP site. Cre is a recombinase encoded by bacteriophage P1 and has suggested implications in cyclization of the genome and dealing with dimeric chromosomes formed during DNA replication. (30) The Cre recombinase binds to the thirty-four base pair loxP site by the binding with two fourteen base pair long recombinase binding elements (RBE) centered on a six base pair crossover region. (30) At each site two Cre complexes bind and cleave the DNA in the crossover region by phosphoryl transfer strand exchange. (30) The cleaved strand can then participate in crossing over and the new strands are ligated together.

The discovery of high levels of antisense transcription at specific meiotic genes that changes during the two life cycles in *S. pombe* gives rise to the hypothesis that antisense transcription acts as a mechanism to regulate these genes. The antisense transcripts are suggested to be involved in the RNAi pathway by hybridization with the complementary sense

transcript. The dsRNA formed is degraded by the yeast double strand ribonucleases and consequently the gene is regulated. To investigate the hypothesis transcriptional analysis was done by qPCR experiments and an in vivo method utilizing a Cre-LoxP recombination to changed expression from one fluorescent protein to the other.

Materials and Methods

In Vitro Assay

Time Course:

Yeast strains in Table 1 were grown in YES at 25 °C to inoculate 500 mL cultures of temperature sensitive stains and 100 mL cultures for non-temperature sensitive strains. The cultures were inoculated in YES at 35°C to be OD 0.10 and placed into a 35°C water bath. Throughout the time course cultures were kept at typical logarithmic growth concentrations. Duplicate samples of OD 10 size for each strain were taken at hours 0, 12, 15, 18, 21, and 24 or every six hours for 24 hours. The samples were immediately spun down at 4000 rpm at 4°C, washed with cold, sterile water, dropped into liquid nitrogen, and stored at -80°C.

RNA Isolation:

Yeast samples were thawed on ice and RNA isolation was performed using Invitrogen's TRIzol Reagent and protocol including during lysis, glass beads were added and the suspension was shaken for 10 minutes. From the isolated RNA, the transcripts of Spo6 sense, Spo6 antisense, Ade4 sense, and a no primer control were strand specifically reverse transcribed to become cDNA by Qiagen's QuantiTect Reverse Transcriptase (RT) Kit. A 1:20 dilution of Actimoycin D in water was added to the 900 ng of Template RNA and used in the Genomic DNA Elimination step of the protocol.

RNA Quantitation:

The quantitative amount of cDNA was measured by RT-qPCR using KAPA Biosystems SYBR Fast Universal qPCR Kit. RT-qPCR was performed in triplicate for each RT reaction using 90 ng of cDNA including a background control reaction from the no RT primer control for both Spo6 and Ade4 transcripts. The resulting data was quantized using standard C_T value

calculations, and two methods of five parametric sigmoid curve fitting to approximate the initial fluorescence value.

In Vivo Assay:

Yeast and Bacterial Strain and growth media

Yeast and Bacterial strains are listed in Table 1 with relevant mutations. All yeast were grown in yeast extracts (YES) and bacteria in LB Amp.

Alkaline Lysis MiniPrep

All *E. coli* plasmids were prepped after overnight growth and then alkaline lysis protocol using Solution A (50 mM Tris pH 7-8, 10 mM EDTA, 100 µg/mL RNase A), Solution B (200 mM NaOH, 1% SDS), and Solution C (3 M KOAc >pH 5).

Yeast and Bacterial Transformations

S. pombe transformations were performed using traditional lithium acetate protocol to produce colonies with integrated linear DNA through homologous recombination. Solutions of 10X LiOAc/TE (1.0 M LiOAc, 0.1 M Tris pH 7.6, 20 mM EDTA pH 8.0, 14 mM glacial Acetic acid) and 40% PEG in 1X LiOAc (40% PEG, 1X LiOAc/TE) were used. All colonies were verified by PCR using primers in Table 2.

E. coli transformation was performed using NEB 10β competent cells and a typical heat shock protocol.

PCR-amplification

Invitrogen Q5 high fidelity PCR was used for all PCR in conjunction with a Touchdown protocol with two minute elongation times. All primers for PCR are located in Table 3.

Gibson Assembly:

NEB Gibson Assembly was the method used to synthesize pLD3/pLD4. A combination 0.2-1.0 pmol of purified PCR products of the cassette was added to three fold excess of the vector with 10 µL of 2X Gibson Assemble Master Mix and water up to a total volume of 20 µL. For two fragments the mixture is incubated at 50°C for fifteen minutes and stored at -20°C until the plasmid can be transformed into bacteria.

Spheroplast FACs:

Spheroplast preparation was performed by yeast collection and EtOH fixation. The cells were then put through osmotic stress and cell wall digestion using solutions of 0.6 M KCl, 0.6 M KCl with 1.0 mg/mL lysing enzymes* and 0.3 mg/mL Zymolyase 20T*, 0.1 M KCl 0.1% triton-x-100, and 20 mM Tris-HCl, 5 mM EDTA pH 8.0. The samples are then incubated with RNase A overnight at 37°C. The cells are spun down, cooled at -20°C for eight minutes, and sonicated using a 3 mm micro tapered tip at output 5 for seven seconds. After sonication 300 µL of the spheroplasts are dyed with 300 µL of 2.0 µM Sytox* dye in FACS sheath fluid. The dyed cells are vortexed and analyzed by flow cytometry.

*Lysing enzymes: Sigma "Lysing Enzymes from *Trichoderma harzianium*"
*Zymolyase: US Biological Zymolyase 20T
*Sytox Dye: Invitrogen Sytox Green nucleic acid stain 5 mM in DMSO

Yeast Mating and Spore Selection:

Yeast mating was performed on ME and sporulated yeast cells were digested overnight in 1:100 dilution of glusylase in water. On YES, 500, 5000, and 50000 spores are plated and then replica plated at YES again and then on selective media. The genotype of the spores were characterized by PCR amplification.

Design of the Two Color Transcription Reporter Cassette:

The strain was developed by mating one strain that has a Cre recombinase integrated at the Spo6 locus after the promoter either in the Sense and Antisense directions with another strain that has a RFP/GFP cassette with integrated LoxP sites at Leu1. The Cre integrated strains were developed by transforming a PCR-amplified Ura5 + Lys7 cassette from plasmid pFS385 using oligonucleotides LD99, and LD100 into yFS808, an Ura4$^-$ Lys$^-$ background strain at the Spo6 locus after the promoter region. The new strain yLD124 was transformed with either PCR-amplified sense Cre cassette using LD86 and LD87 or PCR-amplified antisense Cre cassette using LD88 and LD89 to knockout the Ura5 + Lys7 cassette at the Spo6 locus. This was repeated to produce strains with integrations at Spo4 and Mde2.

The complimentary strain containing the RFP/GFP cassette was created by integrating the cassette at the Leu1 genomic locus of wild type strain yFS104. The RFP/GFP cassette was PCR-amplified with RH16 and RH19 and a vector containing Leu1 and an adh1 promoter was PCR-amplified from plasmid pFS181 using RH20 and RH21. The two PCR products were PCR-amplified, annealed, and ligated using New England Biolab's Gibson Assembly to place the RFP/GFP cassette under the control of the adh1 promoter. The new plasmid has transformed into 10β-competent *E. coli* cells. The transformed bacterial cells were grown up and digested using Xho1 to cut the plasmid in the coding sequence of the Leu1 region. The new DNA fragment was transformed into wild type yeast yFS104 to integrate the plasmid through homologous recombination at the genomic Leu1 locus.

The two strains of sense and antisense integrated Cre strains were mated with the RFP/GFP integrated strain to produce a single strain that has both cassettes. The resulting strain can then be mated with Pac1-TS, Dcr1Δ and the double mutant to produce the experimental strains.

Results

In vitro Relative mRNA Analysis:

To investigate that the hybridization of sense and antisense mRNA transcripts play a role in gene regulation of specific meiotic genes in *S. pombe* transcriptional analysis was performed. The first section of Table 1 lists the *S. pombe* strains and corresponding mutations that were used in the time courses and consequent mRNA isolation, RT, and qPCR. yFS105 was used as a wild type control to compare the change in transcript levels of sense and antisense at Spo6. To eliminate and inactivate the two fission yeast ribonucleases that would degrade any double stranded mRNA transcripts the strains with Dcr1Δ and/or Pac1-TS (Pac1-Temperature sensitive, Pac1 was not deleted because of its biologically essential roles) background were chosen. The involvement of Mie4 was also investigated with a parallel time course.

The specific mRNA transcript levels were quantized by manipulations of the quantification curves and Ct values generated from each time course. Three manipulations were performed on the data to address the relative transcript levels. Typical Ct value calculations were performed by calculating ΔCt where the Ct value for each triplicate was averaged and subtracted from the Ade4 sense values. The relative mRNA concentration difference between samples was calculated by taking the inverse base 2 log of the values and then the reciprocal. The background was subtracted from the no RT primer controls of Spo6 and the data presented in terms of values relative to Spo6 sense at zero hours as in Figure 7C. The remaining two manipulations were performed by five parametric sigmoid curve fittings on the fluorescence data from all forty cycles and the analysis was repeated on a subset of the data, Figure 7A and Figure 7B. The subset of data for the second sigmoid approximation was determined by the local

minimum of plots analogous to Figure 8 that were generated for each qPCR sample. Figure 8 was generated by performing the same five parametric sigmoid curve fittings on 40 cycles and subtracting one cycle from 40 cycles down to 20 cycles. The corresponding number of cycles to the local minimum of Figure 8 dictated the "cutoff" sigmoid approximation where only cycles less than and equal to the value were used. For both methods of sigmoid approximation the values were averaged, normalized to Ade4 sense, background subtracted, and presented relative to Spo6 sense levels at zero hours.

After analysis and comparison to the quantification curves of the three manipulations, the Ct value manipulation best represented the data and was the analysis primarily used. Figure 9 was one control performed to demonstrate that relative transcripts of the wild type strain is reproducible between experiments.

The results from one time course is plotted in Figures 10 and 11 showing the relative mRNA of sense and antisense Spo6 transcripts relative to Spo6 sense at time zero for Wildtype, Pac1-TS, and Pac1-TS; Drc1Δ. Each sample was normalized to an endogenous gene, Ade4 sense which is expected to be transcribed consistently throughout the experiment. The background was subtracted by a no RT primer control for both the sense and antisense transcripts. Figure 10 shows transcript levels for each strain during the course of the experiment with relative amount of transcript versus hours at the no permissive temperature. The plot representing Wildtype only shows samples for 0, 12, and 24 hours because no significant change is expected in the transcriptional profile.

The resulting plots show a trend in the three strains, Wildtype, Pac1-TS, and Pac1-TS; Dcr1Δ of increasing relative sense and antisense transcript levels over the course of the experiment. The data shows limited evidence for either case that antisense transcription is

involved in gene regulation by the formation of dsRNA or not. The plots illustrate an increase in sense transcripts as expected with the inactivation of the ribonucleases showing that the ribonucleases are involved in the degradation of the sense transcripts. In addition, the plots also show a consistent increase in the antisense transcript as well.

To further address the qPCR data the plots in Figure 11 were displayed to show the change in transcription of sense and antisense Spo6 transcripts between strains. In comparison of Pac1-TS and Pac1-TS; Drc1Δ, the double mutant would be expected to show increased sense transcription when compared the single mutant and an even greater difference when compared to the Wildtype strain. The data does not represent such a phenomena but suggests a general trend of increased transcription in all strains. In both Figures 10 and 11 there is a general trend for an increase in both sense and antisense transcripts across all three strains. The transcriptional assay remains unconvincing and further investigation is needed to show a biologically more complex mechanism can be involved with antisense transcription in gene regulation.

In vivo Assay Design:

Addressing the possibility of indirect antisense transcription involvement in gene regulation was investigated by the model presented in Figure 12. The development of the assay began with the construction of the integrated reporter cassette in Figure 13A. A 3662 bp fragment of pFS387 and 5280 bp fragment of pFS181 diagramed in Figure 14A and 14 B were PCR amplified using primers RH16/RH19 and RH20/RH21. Amplifications of the two cassettes shown in Figure 15 were used in Gibson assembly to anneal and circularize them into pLD3/pLD4, Figure 14C.   The plasmid was transformed into E. coli which was selected against the AmpR gene on the plasmid. Verification of the transformed E. coli was validated by alkaline lysis miniprep and restriction digest using ClaI and ApaLI with expected fragments of 4369 bp,

2622 bp, 1245 bp, and 497 bp seen in Lanes 2 of Figure 16. pLD3/pLD4 was isolated, digested

with Xho1, and transformed by homologous recombination at the genomic Leu1 locus of

yFS104.

The integration of pLD3/pLD4 at Leu1 in Figure 13A would make yFS104 Leu1 positive

by the recombination with the endogenous Leu1-32. The strain did not become Leu1 positive

and needs to be sequenced to confirm two mutated Leu1 cassettes present. The transformation

colonies were verified by and PCR amplification with LD1/LD2, RH26/RH27, RH26/RH28,

RH27/RH29, and RH28/RH29 in Figure 17. In Figure 17, Lanes 1, 3, 5, 7, 9 and 2, 4, 6, 8, 10

represent two identical PCR sets for two transformation colonies. The odd numbered lanes

represent a failed integration and the even lanes represent a positive integration. The even

numbered lanes 2, 4, and 10 represent positive PCR control (470 bp) and integration at the

upstream and downstream Leu1 sites (1808 bp and 2122 bp). Lanes 6 and 8 show the negative

control for plasmid integration with no band observed and no product for the total length of the

transformed locus due to the length, 10612 bp. To further verify the RFP/GFP integration into

the yeast genome the colony was examined by fluorescent microscopy in Figure 18. The three

images show a Dapi, GFP, and RFP image for the cells showing the auto-fluorescence of the

yeast cells, no expression of GFP or bleed through from the red channel, and expression of RFP

as expected. The yFS104 plus RFP/GFP strain will then be mated with strains with integrated

Cre genes to produce strains that contain both integrations.

The demonstration of the RFP/GFP cassette recombination with the Cre LoxP

recombinase mechanism to change the fluorescent protein expressed is in progress. The

recombination will be shown by transforming pFS240 or pFS241 in Figure 19 into the yFS104

plus RFP/GFP strain. The Cre recombinase in the plasmid is under the control of an nmt1

promoter that will express Cre and change all transformants from the expression of red fluorescent protein in yFS104 plus GFP/RFP to green fluorescent protein. The colonies of the transformation are screened using a fluorescent dissecting microscope and final verification of the recombination will be performed by sequencing.

With the proof of the RFP/GFP reporter cassette recombination working, the second design of the assay was to develop strains where Cre recombinase was integrated both sense and antisense in place of Spo6, Spo4, or Mde2. The endogenous gene was removed by a transformation of yFS808 with pFS385 (Figure 20), an Ura5 and Lys7 gene to make yFS808 Ura5 Lys7 positive in Figure 13B. The colonies were selected for using positive selection for the Ura5 and Lys7 integration. PCR amplification of pFS385 in Figure 20 was done using RH33/RH34, RH49/RH50, and RH51/RH52 for the genes respectively. The replacement of Spo6 was verified by PCR with LD1/LD2, LD101/LD140, and LD140/RH22 in Figure 21. Similarly the replacement of Spo4 in two colonies was confirmed with LD1/LD2, RH36/RH37, RH09/RH37, and LD101/RH37 in Figure 22. The double band appearing in lane two and five were evidence of the transformation yielding a heterozygous diploid for the two colonies selected. This was confirmed by Speroplast FACS in Figure 23. The transformation for the replacement of Mde2 is in progress along with the subsequent transformations with pFS378.

To this point the knockout of Spo6 and Spo4 have been performed and integration of the reporter cassette at Leu1. The knockout of Mde2 is in progress along with the integrations of sense and antisense Cre. Once the Cre gene is integrated in the proper orientations and locations the strains will be mated to the strain with the RFP/GFP reporter cassette. The mating will be performed by sporulation and random spore selection to produce the testing strains. The testing

strains can then be mated with Pac1-TS and Pac1-TS; Dcr1Δ mutant strains to contrast the results if the transcriptional analysis.

Once all three strains with the replacement of either Spo6, Spo4, or Mde2 are transformed, the following transformation is performed twice, once with pFS378 in Figure 24 PCR amplified with LD86/LD87 and again with LD88/LD89. The resulting integration is represented in Figure 13C and 13D with sense and antisense integration of an unmarked Cre recombinase gene. The six resulting strains are then to be mated with the yFS104 plus RFP/GFP strain, put through sporulation, and random spore selection to make the testing strains. The testing strains can then be used for experiment and to be mated with yFS787 and yFS118. With the final experiments assaying for radial sectors of green fluorescent colonies which are indicative of relative sense transcripts.

Discussion

Gene regulation is an important biological function that is ubiquitous in cells of every organism for maintaining homeostasis and moderating cell activity. Of the many mechanisms of gene regulation, antisense transcription is proposed to be relevant by the pairing with the complimentary mRNA transcript thereby inhibiting translation or initiating degradation. RNA sequencing data performed on fission yeast showed elevated antisense transcription levels at a specific group of genes. (22) A subset of the meiotic *S. pombe* genes maintained this characteristic elevated antisense transcripts during mitotic growth but the relative sense and antisense transcripts changed dramatically during the meiotic life cycle. To address whether antisense transcription of certain meiotic genes has implications in gene regulation by preventing entrance to a meiotic life cycle during vegetative growth, transcriptional analysis of mRNA concentrations was performed and a dual fluorescent protein assay was designed.

To address mRNA transcriptional levels, strand specific qRT-PCR was performed on the gene Spo6. Spo6 was a gene that had previously been identified to have elevated antisense transcripts that changed when the yeast life cycle changes. The qRT-PCR samples were taken using yeast strains that had neither, one, or both of the *S. pombe* double stranded ribonucleases inactive. The suppression of the two ribonucleases would allow the concentration of dsRNA to increases constantly for specific sequences that are the result of hybridization of the sense and antisense transcripts. The ribonucleases Dcr1 and Pac1, if active, would degrade the dsRNA acting to regulate the expression of the meiotic gene in question. Dcr1Δ was used because it was previously shown to lead to no major change in the transcriptional profile. On the other hand, a temperature sensitive allele of Pac1 was used because Pac1 is an essential gene and important in the processing of snRNA.

After the qRT-PCR quantification was collected and analyzed, the resulting data displayed relative sense and antisense Spo6 transcripts. The transcriptional assay remains unconvincing and further investigation is needed to show the biologically more complex mechanism involving antisense transcription in gene regulation.

One of the limits of the qPCR technique that accounts for the variability and less than convincing data is the restriction by the low concentration of sense transcript present. The detection of such low concentrations leads often to negative qPCR quantification analyzes and makes the data inconclusive as it does not accurately represent the biological activity of the cells. The need for a more sensitive assay lead to the development of the in vivo assay using the RFP/GFP reporter cassette.

With the inconclusive data associated with transcriptional analysis another assay was designed so show that a biologically more complex mechanism was at hand involving antisense transcripts and gene regulation. The schematic laid out in Figure 12 demonstrates the design of the assay. To show similarly how sense transcript levels change in vivo, a Cre-LoxP recombination with a RFP/GFP cassette was used. The Cre protein was to be integrated both sense and antisense direction as an unmarked cassette in the place of the gene of interest, in this case Spo6, Spo4, and Mde2. Once integrated, the new strains with Cre would be mated to the strain with the RFP/GFP reporter cassette at Leu1. The resulting new strain can be tested to show relative sense transcripts by counting the radial green fluorescent sectors of colonies under a fluorescent dissecting microscope that are indicative of the recombination of the reporter cassette by Cre recombinase to produce GFP instead of RFP.

The investigation of antisense transcription forming dsRNA duplexes with their complementary sense transcripts was addressed by this assay. In vivo, the RFP/GFP reporter

cassette will be able to show if the hybridized sense and antisense transcripts participate in the

gene regulation pathway via RNAi which is key to understanding how some genes may be

regulated. Evidence for the RNA duplex formation cannot be made purely on the qPCR data due

to its inconclusive and variable nature, but the in vivo assay, demonstrated by the fluorescent

color change in the RFP/GFP reporter cassette with the Cre LoxP recombination, may allow for

the sensitivity that is needed. The design of this assay is hinged on the premise that the

expression of the Cre recombinase protein once expressed will come in contact with the LoxP

sites and the expression of the fluorescent proteins. The design also assumes that the integration

of Cre recombinase protein does not alter the transcriptional profile of any of the genes of

interest so that Cre is expressed in the same manner as if the endogenous gene remained under

the control of the promoter. Maintaining these two assumptions that the transcriptional profile

does not change and the Cre recombines the cassette, this assay can be applied to any

transcriptional investigation. The incorporation of the Cre-LoxP recombination and the

RFP/GFP cassette is a powerful and sensitive tool that can address transcriptional analysis by

simple monitoring of change in fluorescent profile. This being true, the in vivo assay with

continued investigation will lead to insight into more comprehensive understanding of regulatory

pathways of the cell and potential for new ways to artificially regulate gene expression.

Figures

A

Pac1-TS F_0

B

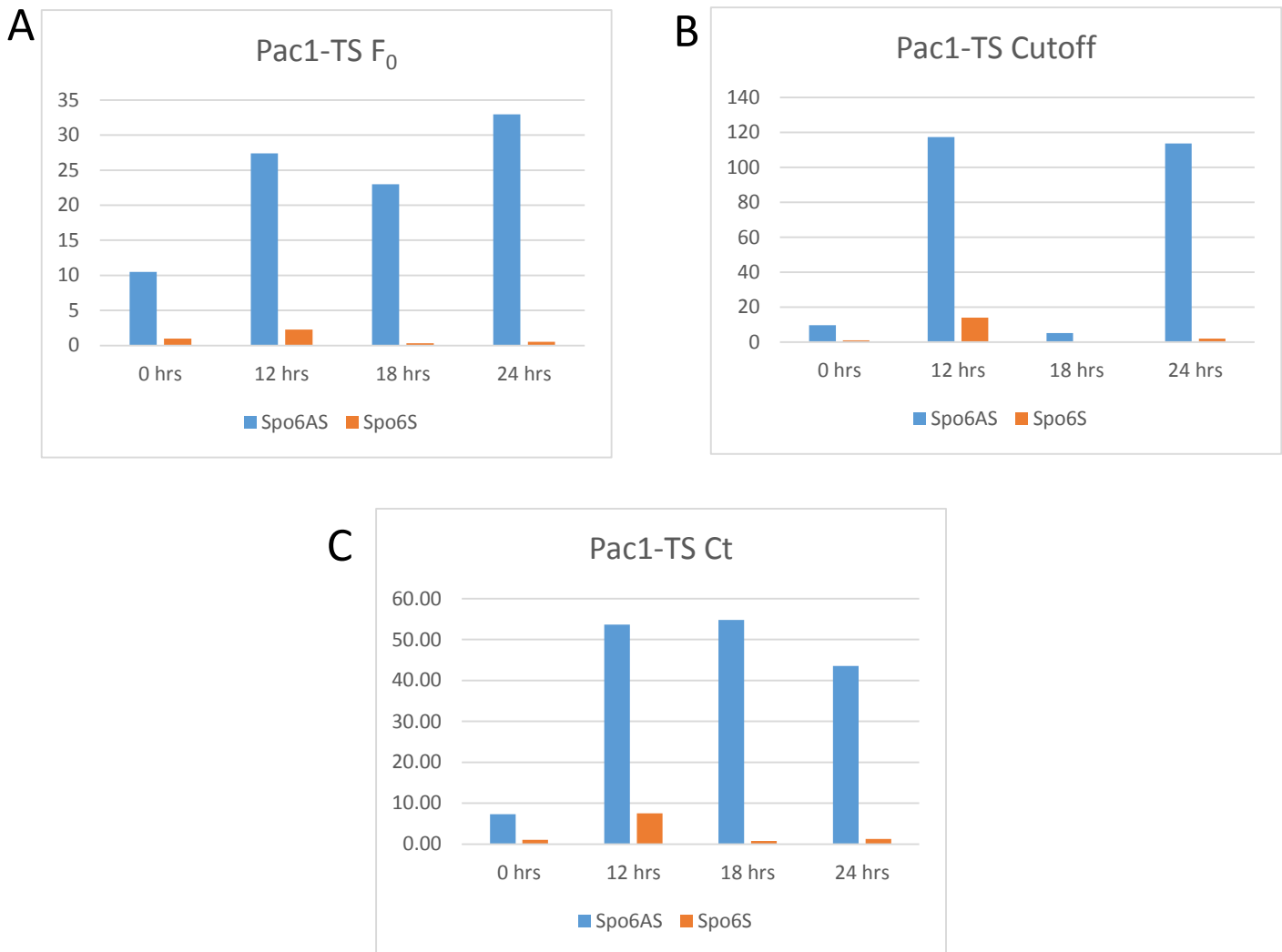### Pac1-TS Cutoff

C

Pac1-TS Ct

Figure 7: Sample qPCR Data Interpretations:

The three plots display qPCR data of Pac1-TS with three different calculations of Spo6 Sense, in orange and Spo6 Antisense, in blue. The Spo6 mRNA transcripts are relative to Spo6 Sense at zero hours for all four time points. (A) Using a five parametric sigmoid curve approximation of the mRNA at cycle zero for all forty cycles of qPCR data. (B) Using the cutoff approximation with a subset of the forty cycles of qPCR data as described in R. G. Ruteredge's Paper (25). (C) Typical Cutoff threshold approximation using delta Ct values.
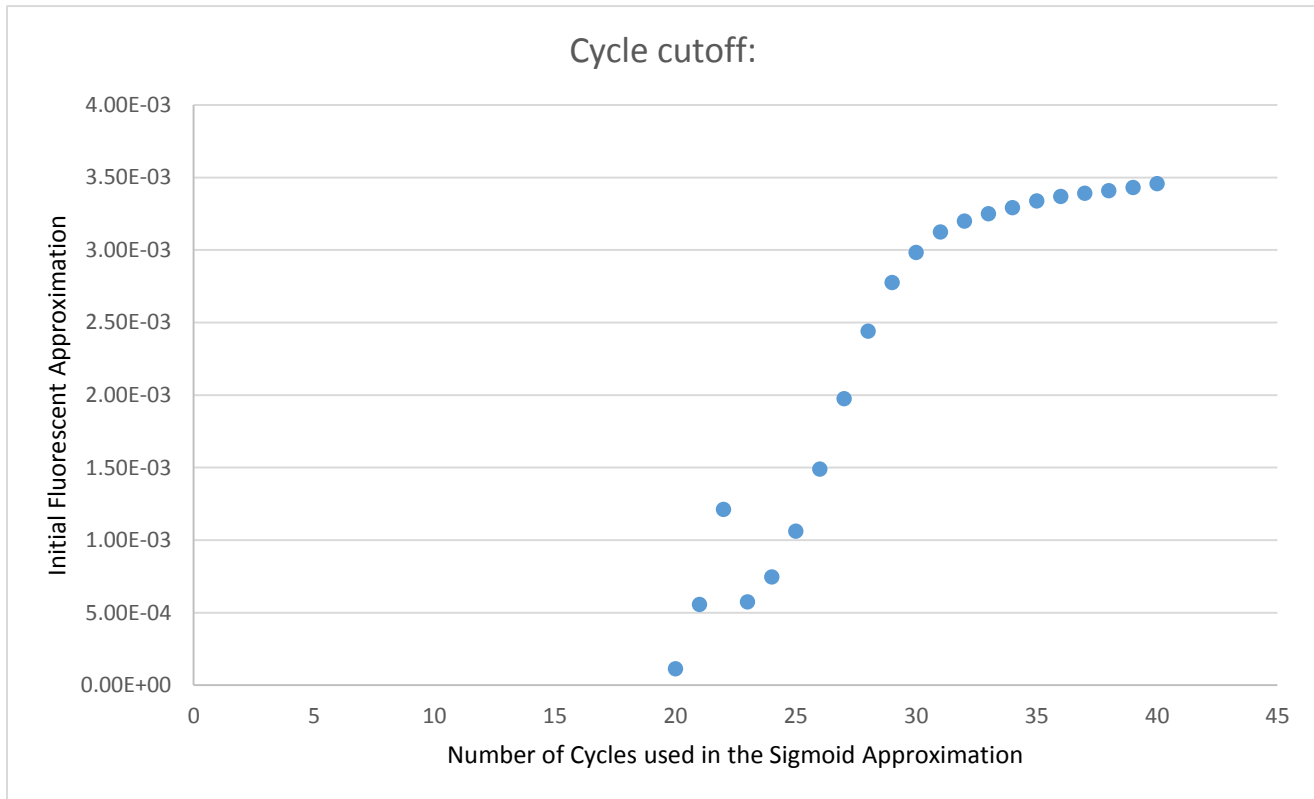
Figure 8: Determination of Cycle Cutoff Approximation

The plot above shows how the subset of qPCR data is determined. The quantification data is taken and five parametric sigmoid curve approximations are performed on the full 40 cycles and consequently N - 1 cycles from forty down to twenty cycles. The local minimum of the approximations versus the corresponding number of cycles, in this case at 23 cycles, represents the best fit of the data.
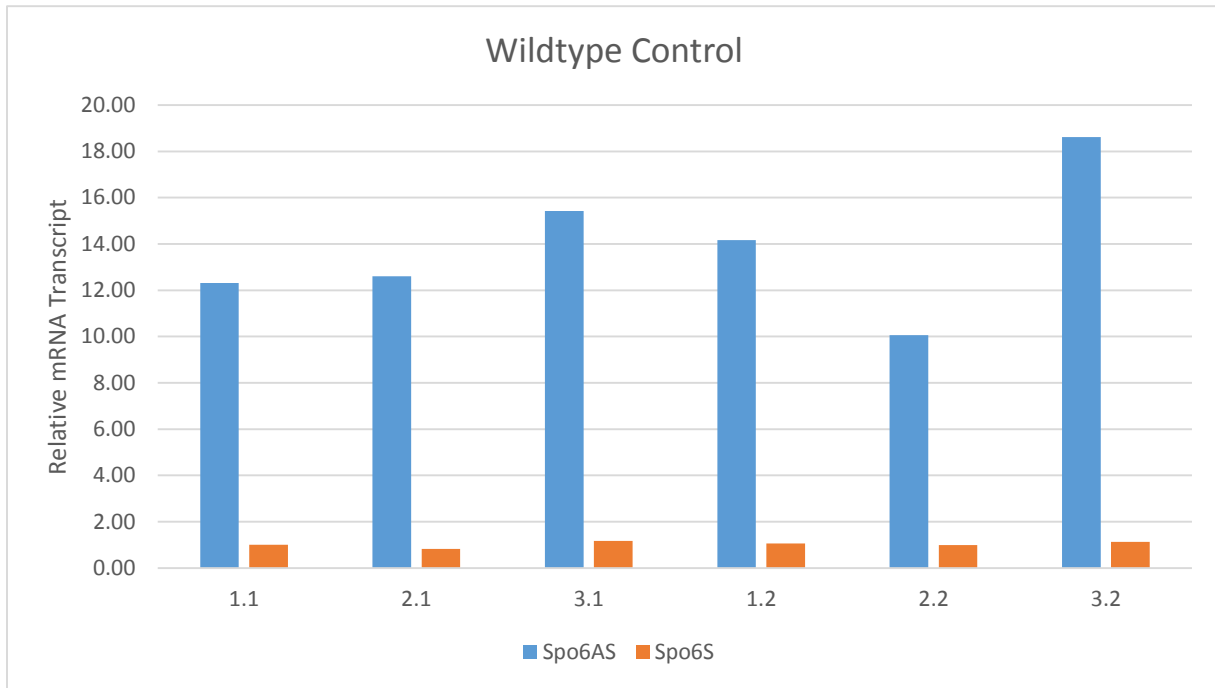
Figure 9: Wildtype Reproducibility Control

Three independent samples of Wildtype in duplicate were taken from mid-log growth cells grown at 30°C. The six samples had Spo6 mRNA Sense and Antisense quantized. The typical calculations for qPCR analysis was performed on the parallel samples showing the reproducibility of the first time point.
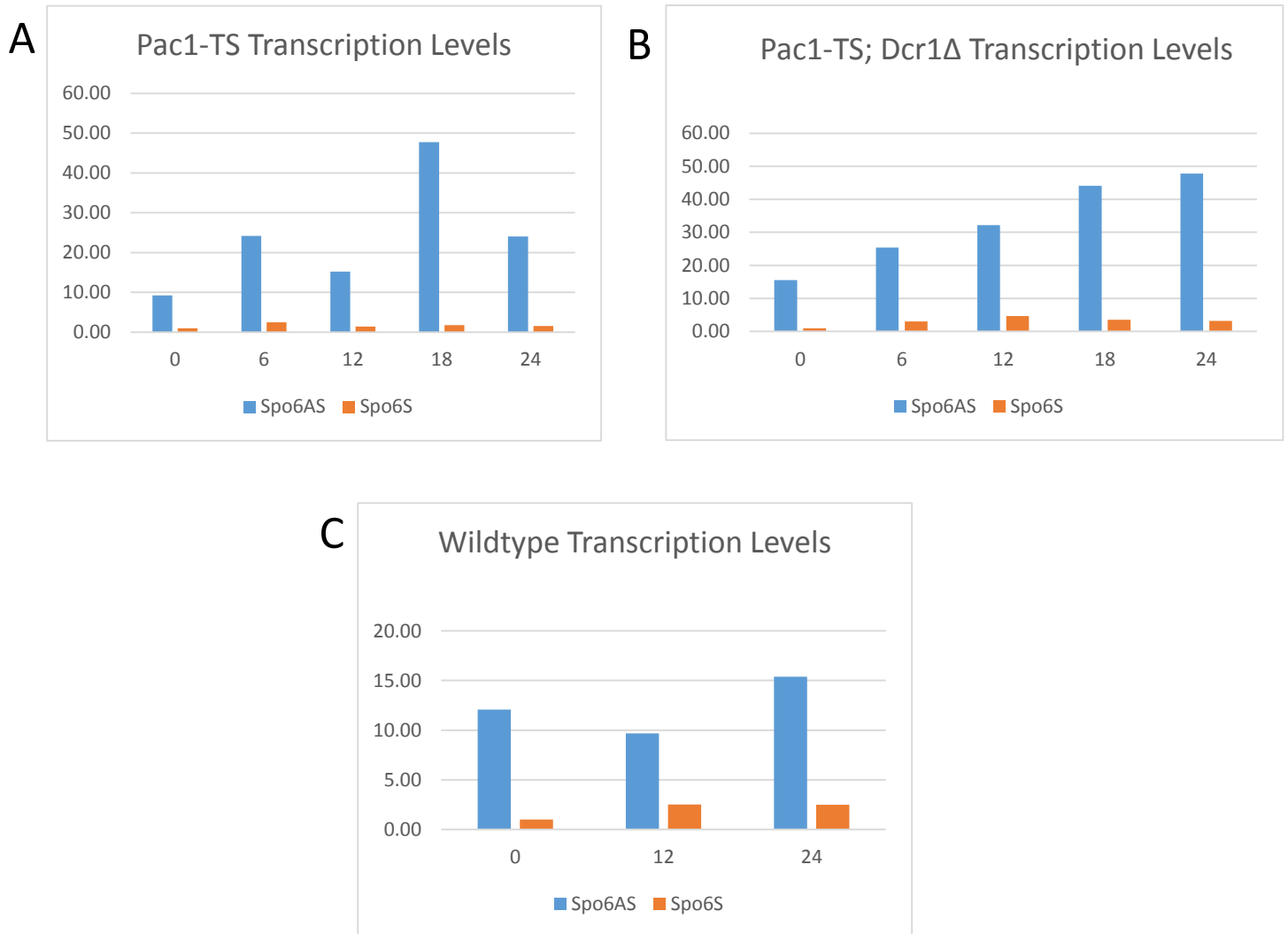
Figure 10: Complete Time Course Analysis for Wildtype, Pac1-TS, and Pac1-TS; Dcr1Δ

Data from qPCR experiments is plotted as antisense signal relative to sense signal for the three strains Wildtype, Pac1-TS, and Pac1-TS; Dcr1Δ. Each plot represents the relative amount of transcript compared to Spo6 levels at zero hours plotted against the time at 35°C in the time course. Sense and Antisense transcript levels for each time point are plotted alongside one another in blue and orange, respectively. A) Wildtype B) Pac1-TS C) Pac1-TS; Dcr1Δ
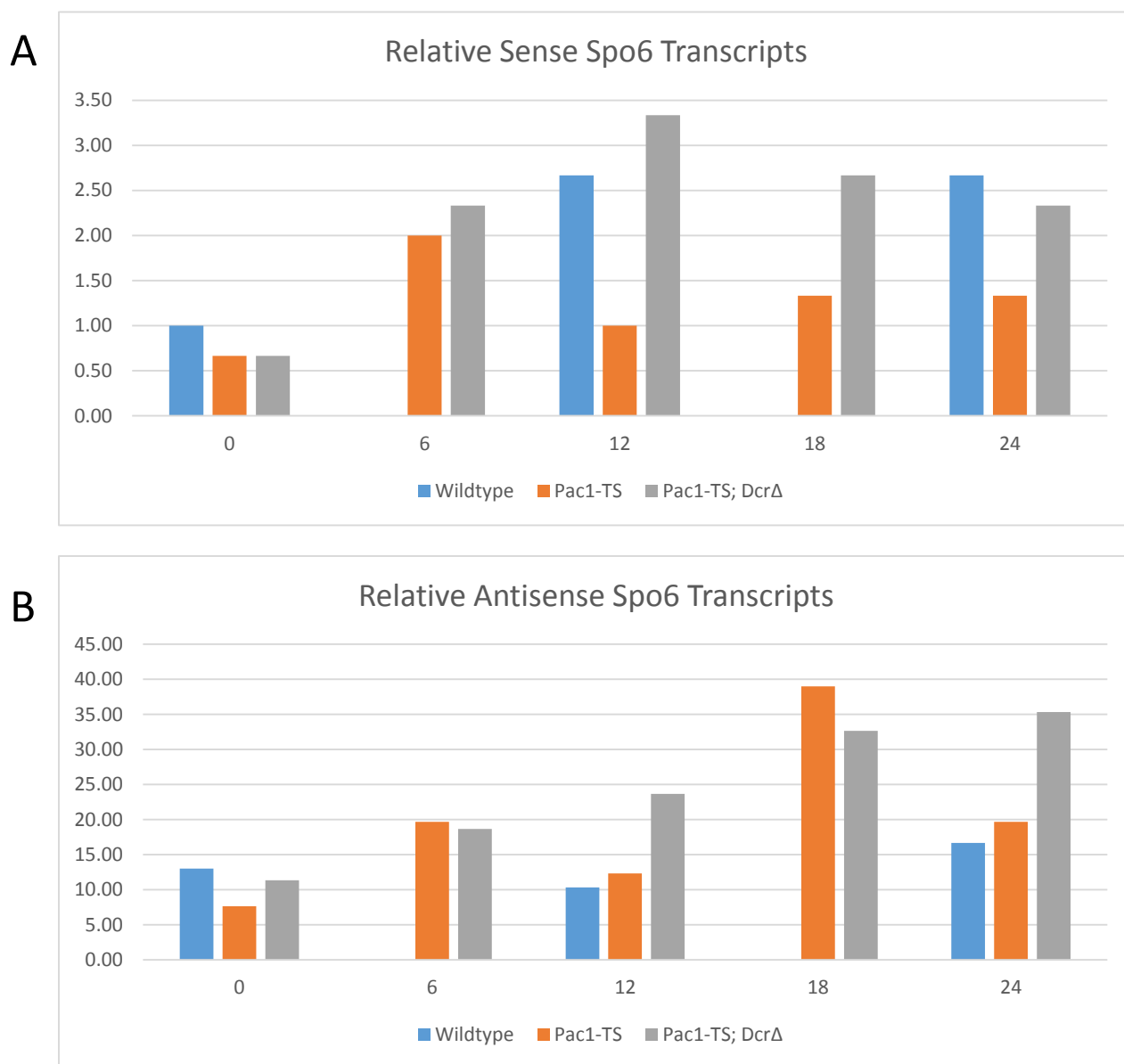
Figure 11: Spo6 Sense and Antisense Transcription between Strains

Presenting plots A), B), and C) from Figure 10 on the same graph gives another perspective on the transcriptional analysis. Time points at six and eighteen hours for Wildtype were not performed as no change in transcription is expected, therefore only Pac1-TS and Pac1-TS; Dcr1Δ are represented.
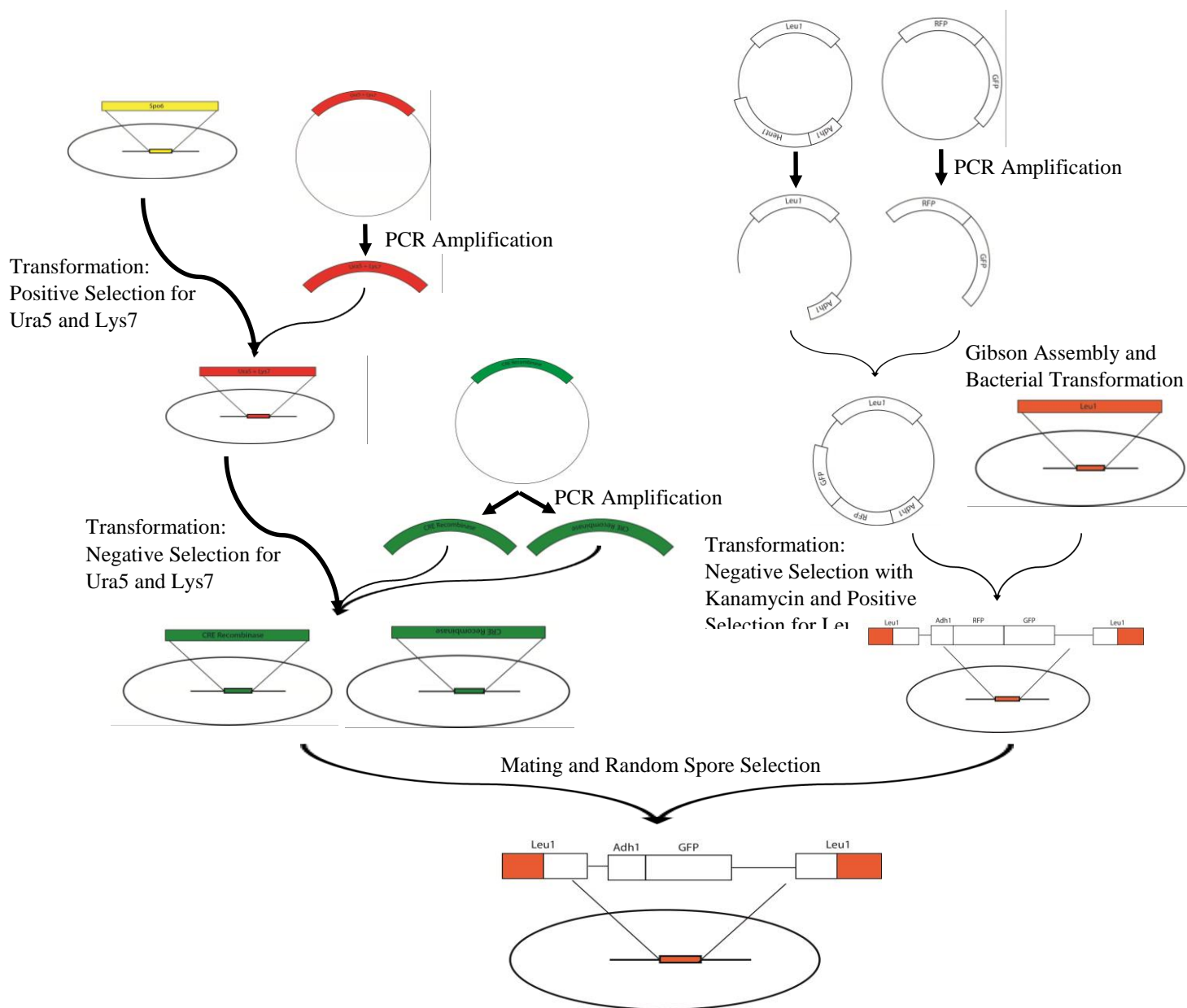
Figure 12: Schematic of In Vivo Testing Strain Design

The diagram illustrates the pathway to develop the In Vivo assay using the RFP/GFP reporter cassette and the CRE LoxP Recombinase system. Beginning on the right branch, the RFP/GFP reporter cassette and a destination vector were PCR amplified. The two fragments were hybridized, ligated, and amplified by NEB's Gibson Assembly. The resulting combined fragments placed RFP under the control of an Adh1 promoter and left GFP unexpressed. The plasmid was transformed into bacteria, and amplified so that it could be linearized and transformed into yeast by homologous recombination at the Leu1 locus. The transformation produces a strain that is Leu$^+$ with Kanamycin resistance, and fluoresces red when excited with 568 nm light. The other branch of the diagram produces the CRE protein. The left branch is the synthesis of an unmarked integration of CRE in the sense and antisense directions in place of Spo6 under the genomic promoter. This is achieved by two transformations, first introducing the Ura5 + Lys7 integration replacing Spo6 and a subsequent transformation to replace it with CRE Recombinase. Once the unmarked CRE is integrated in the two strains, it can be mated with the RFP/GFP reporter strain. Random spore selection will give rise to colonies that have both mutations and can then be used in the assay.
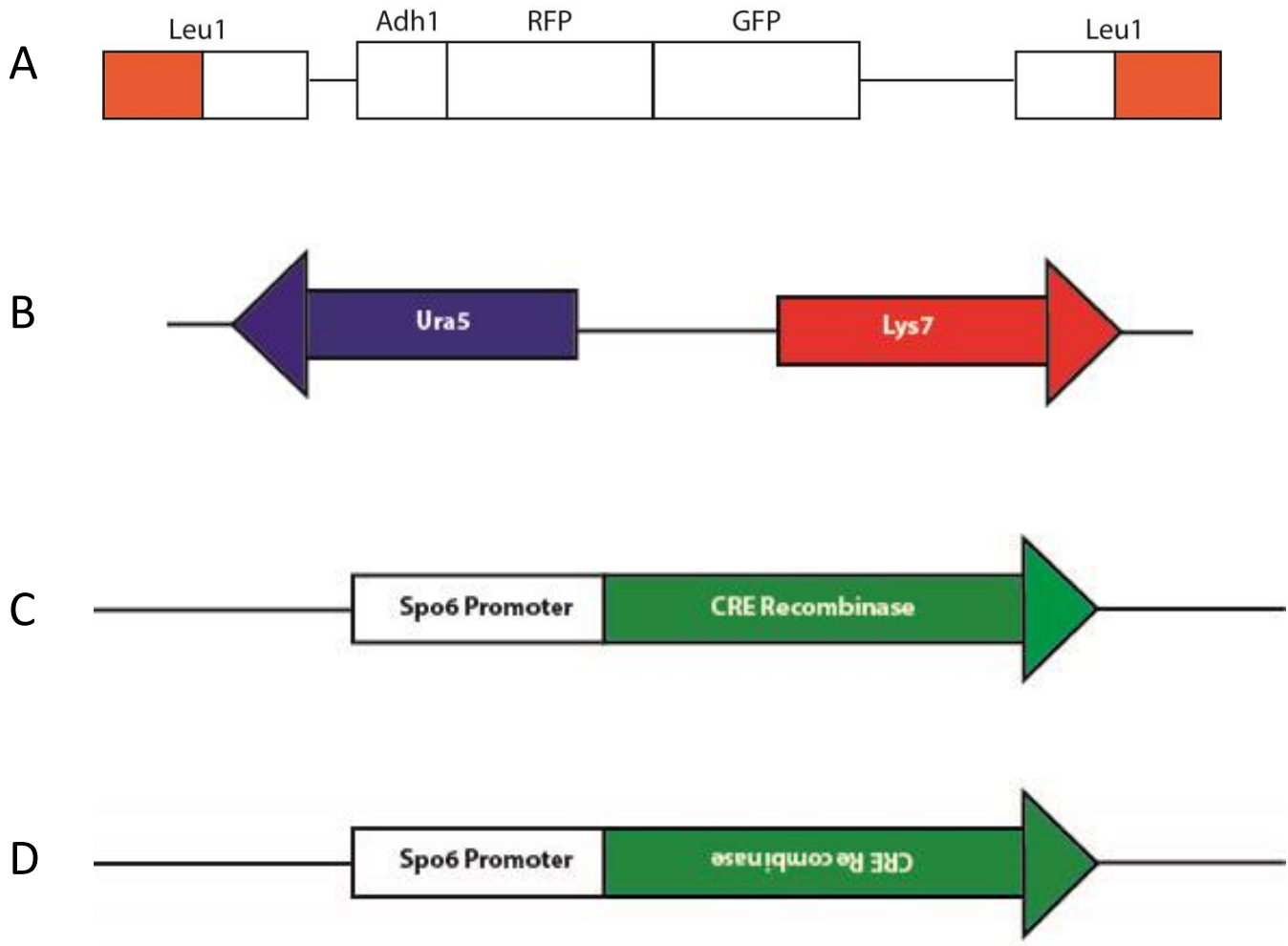
Figure 13: Gene Maps of Transformation Integrations

Diagrams of integrated cassettes achieved by transformations in the design of the in vivo assay.
(A) RFP/GFP report cassette in genomic Leu1 of yFS104. (B) Replacement of Spo6 in yFS808
with Ura5 + Lys7 cassette. (C) Sense Cre integration at Spo6. (D) Antisense Cre integration at
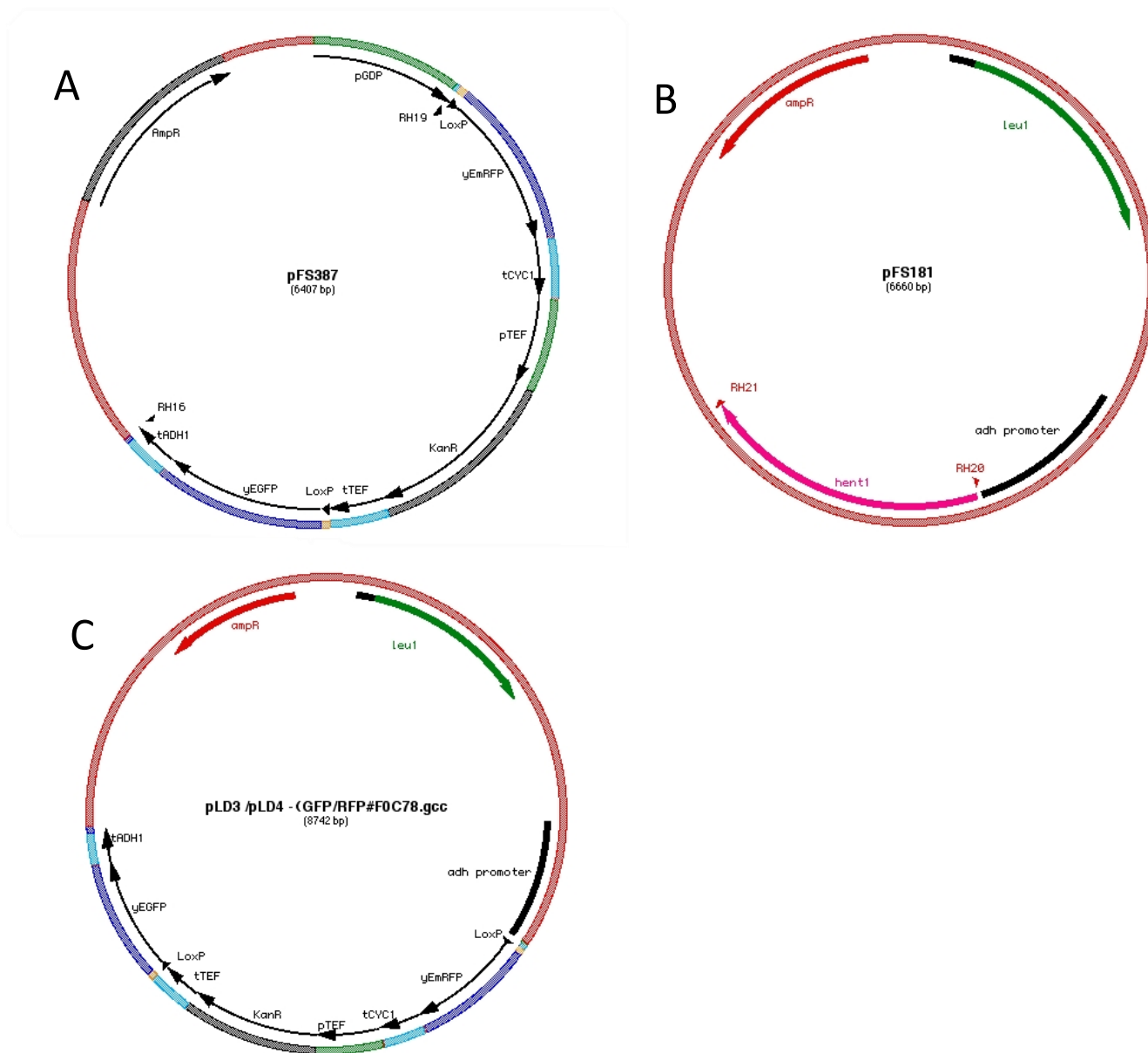Spo6.

Figure 14: Plasmid Maps of pFS387, pFS181, and pLD3/pLD4

Gene maps for (A) RFP/GFP cassette, pFS387, (B) Accepting vector pFS181, and (C) the combination of pFS387 and pFS181 created by Gibson Assembly.
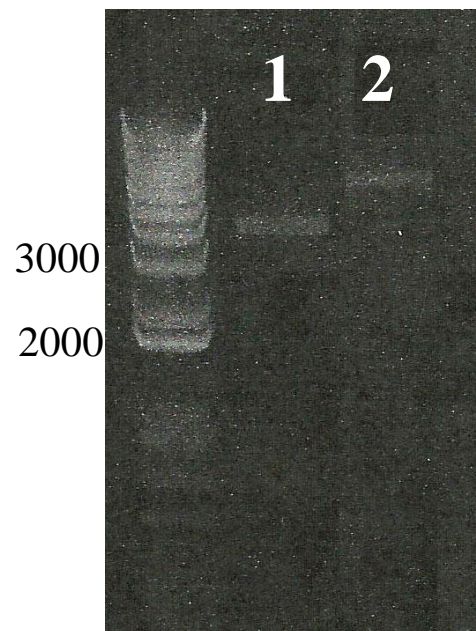
Figure 15: PCR Amplification of two pieces of Gibson Assembly Plasmid

High fidelity PCR amplification of the RFP/GFP construct and a vector containing Leu1 and an Adh1 promoter in Lanes 1 and 2, sizes 3662 bp and 5280 bp.
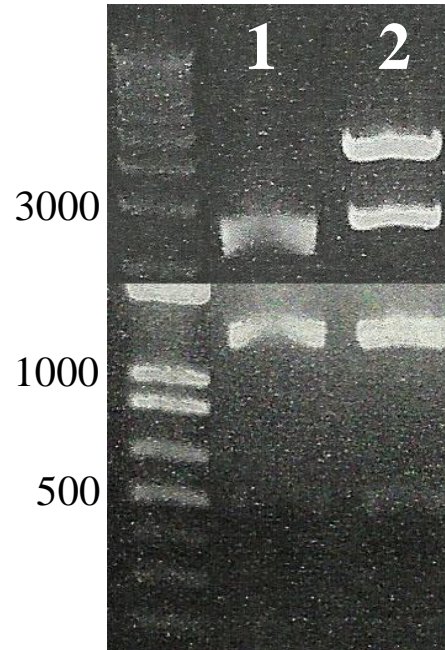
Figure 16: PCR Verification of Transformation of pLD3/pLD4 into E. coli

The two vectors amplified in Figure 14 were annealed and ligated by NEB's Gibson Assembly. The resulting plasmid was transformed in NEB 10β competent *E. coli* cells. The plasmid was negatively selected by using kanamycin (Kanamycin resistance gene located between RFP and GFP). The plasmid was miniprepped and digested using ClaI and ApalI with expected sizes 4369 bp, 2622 bp, 1245 bp, and 497 bp. Lane 1 represents an unsuccessful transformation where not all of the plasmid remained intact. Lane 2 shows the four expected bands for successful transformation.
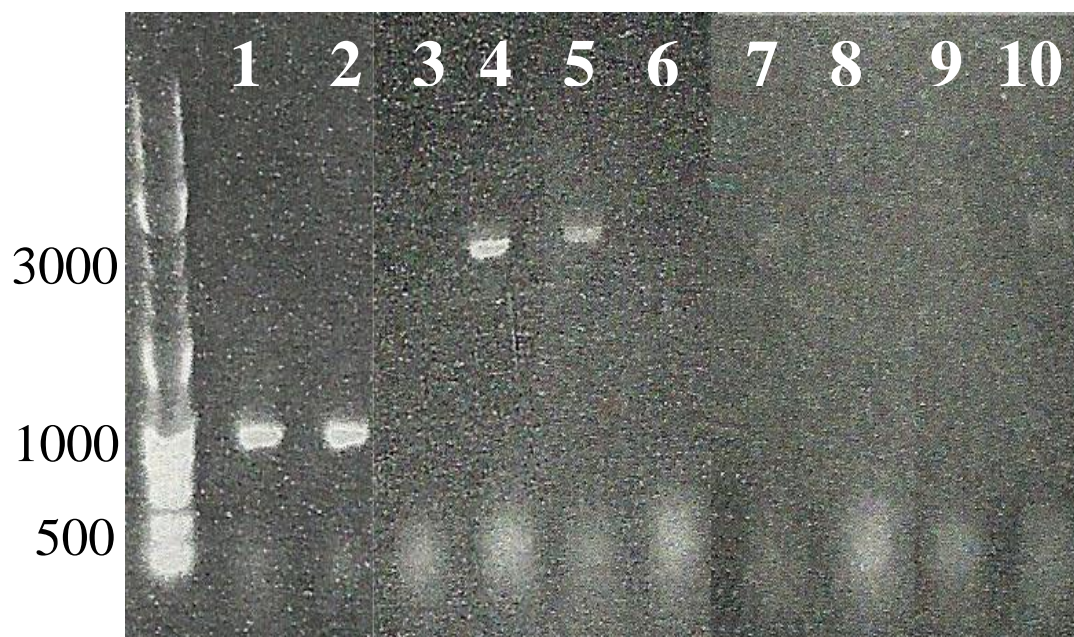
Figure 17: RFP/GFP integration into yFS104

Transformation of the linearized plasmid by digest with Xho1 to place the construct at Leu1 was confirmed by PCR Amplification. Lanes 1, 3, 5, 7, 9 and 2, 4, 6, 8, 10 represent two identical PCR sets for two transformation colonies. The odd numbered lanes represent a negative integration where the construct integrated at another locus while even numbered lanes represent the positive integration at Leu1. Going down the odd lanes, the PCR products represent a PCR control (470 bp), no integration at the downstream Leu1 (no band), a negative integration of the plasmid (2068 bp), product for the total length of the untransformed loci (1867 bp), and no integration at the upstream Leu1(no band). Even Lanes 2, 4, and 10 show positive control (470 bp) and integration at both Leu1 sites (1808 bp and 2122 bp). Lanes 6 and 8 show the negative control for plasmid integration with no band observed and no product for the total length of the transformed locus due to the length, 10612 bp.
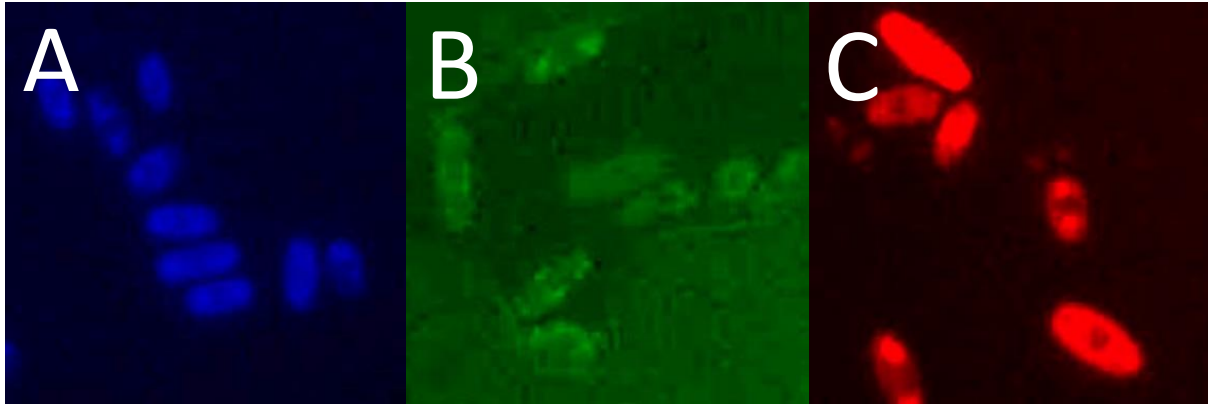
Figure 18: Verification RFP/GFP integration into yFS104 by Fluorescent Microscopy

The integration of the RFP/GFP cassette at Leu1 was confirmed by fluorescence microscopy. (A) A Dapi filter showing the presence of yeast cells. (B) GFP filter shows the negative control and confirms that the RFP has no bleed through in the green fluorescent channel. (C) RFP filter show the expression of the RFP yielding the red fluorescent yeast cells.
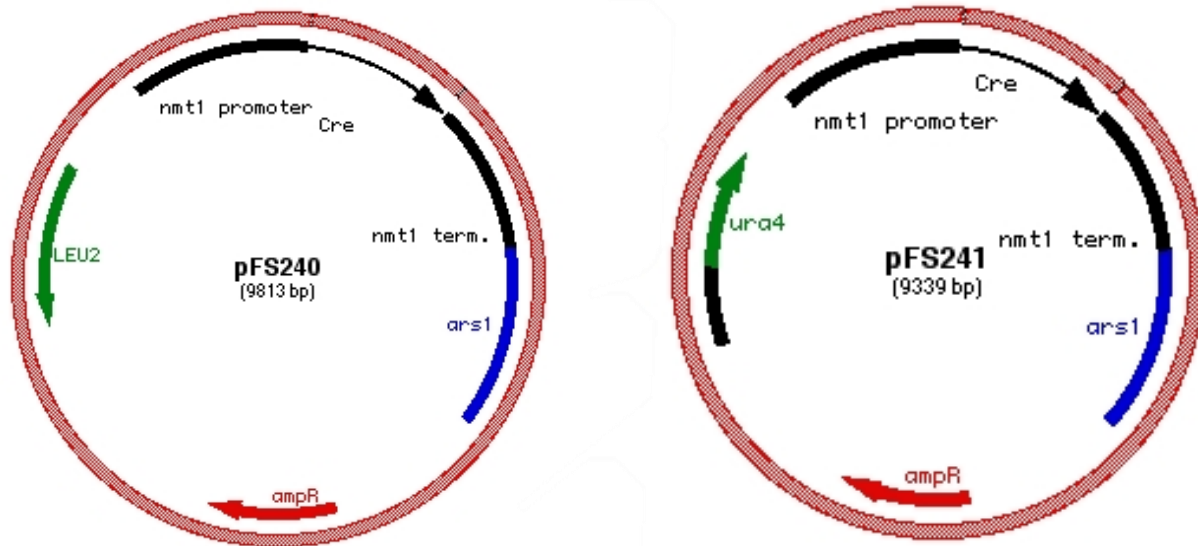
Figure 19: Plasmid Maps of pFS240 and pFS241

Gene maps of pFS240 and pFS241 that will be transformed into yFS104 plus RFP/GFP so show the proper recombination of the cassette and the change from red to green fluorescence..
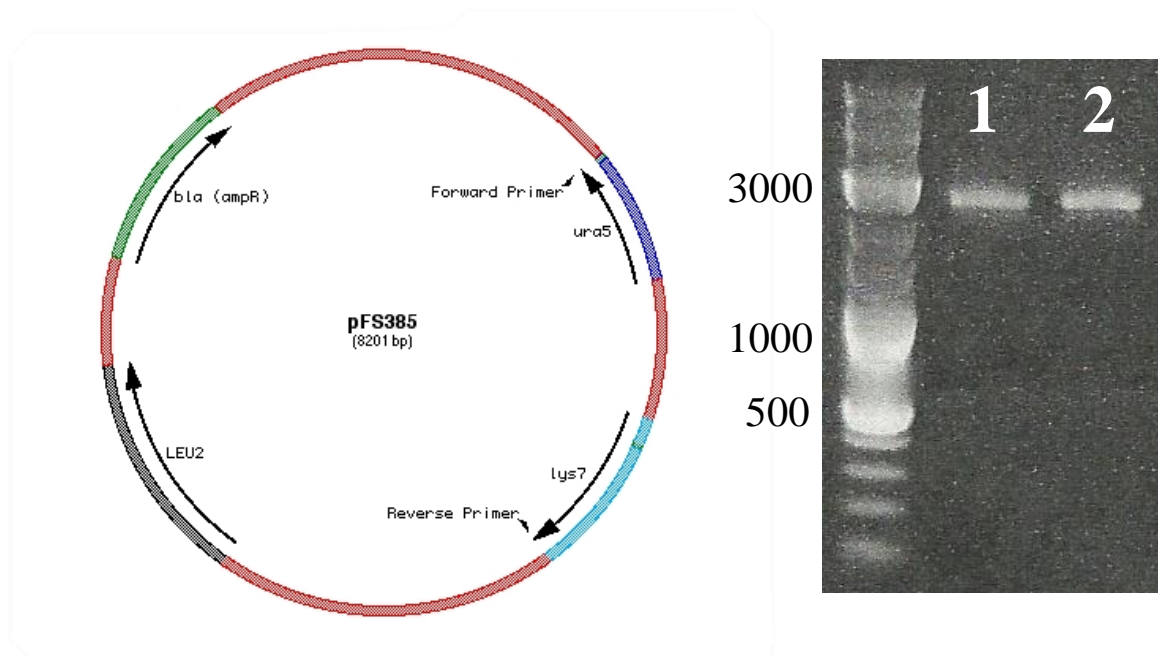
Figure 20: Plasmid Map and Amplification of pFS385

Gene map of pFS385 used for replacement of Spo6, Spo4, and Mde2. pFS385 (Ura5 + Lys7 cassette) amplification is shown for both Spo6 and Spo4 in Lanes 1 and 2 with expected sizes 2500 bp .

Figure 21: Verification of Replacement of Spo6 with pFS385 Cassette

PCR confirmation of integration of the Ura5 + Lys7 cassette at Spo6. Lane 1 is a PCR control from an endogenous loci. Lane 2 and 3 are products from a primer pair inside the transformed cassette and downstream of Spo6 and a primer pair upstream and downstream of Spo6. The expected sizes for the three lanes are 470 bp, 715 bp, and 2074 bp.
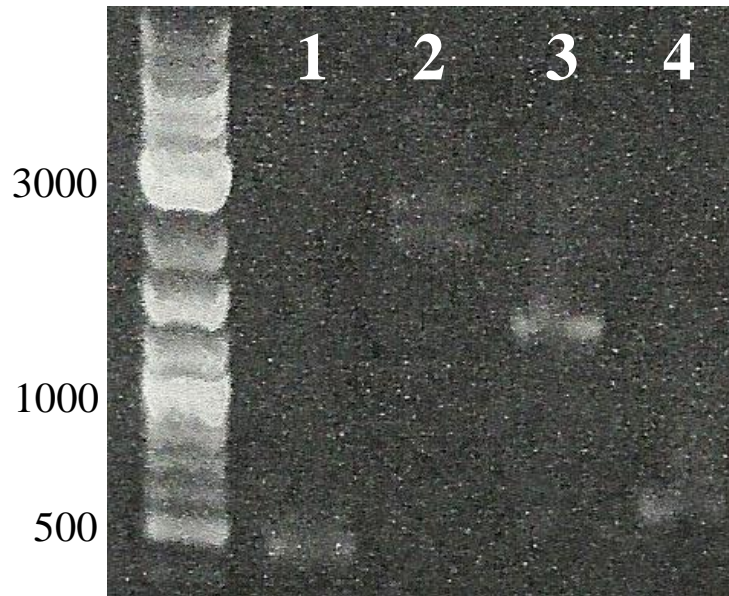
Figure 22: Verification of Replacement of Spo6 with pFS385 Cassette

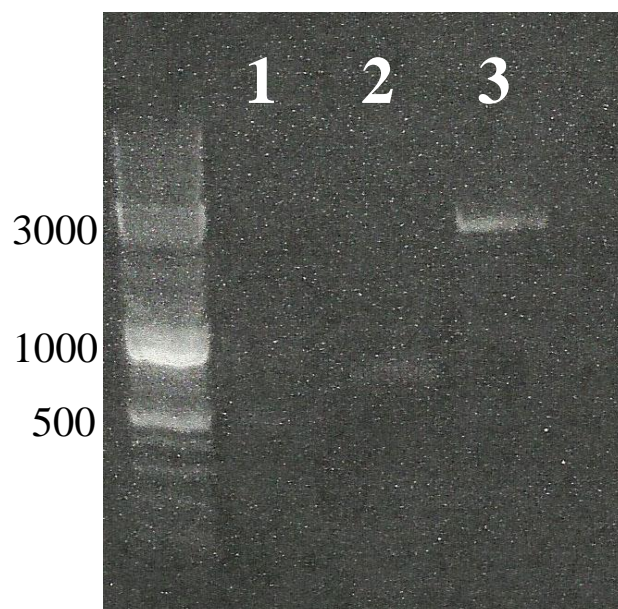PCR confirmation of the transformation of the Ura5 +Lys cassette at Spo4 resulting in diploid sample. Lane 1 is a PCR control (470 bp) and the next lane represents the primer pair upstream and downstream of Spo4, resulting in a double band suggesting a heterozygous diploid transformant (expect one band from genomic locus at 2034 bp and successful transformation at 2495 bp).   Lanes 3 and 4 show integration of the Ura5 + Lys7 cassette and the presence of the endogenous Spo4 gene with expected sizes 1341 bp and 584 bp.
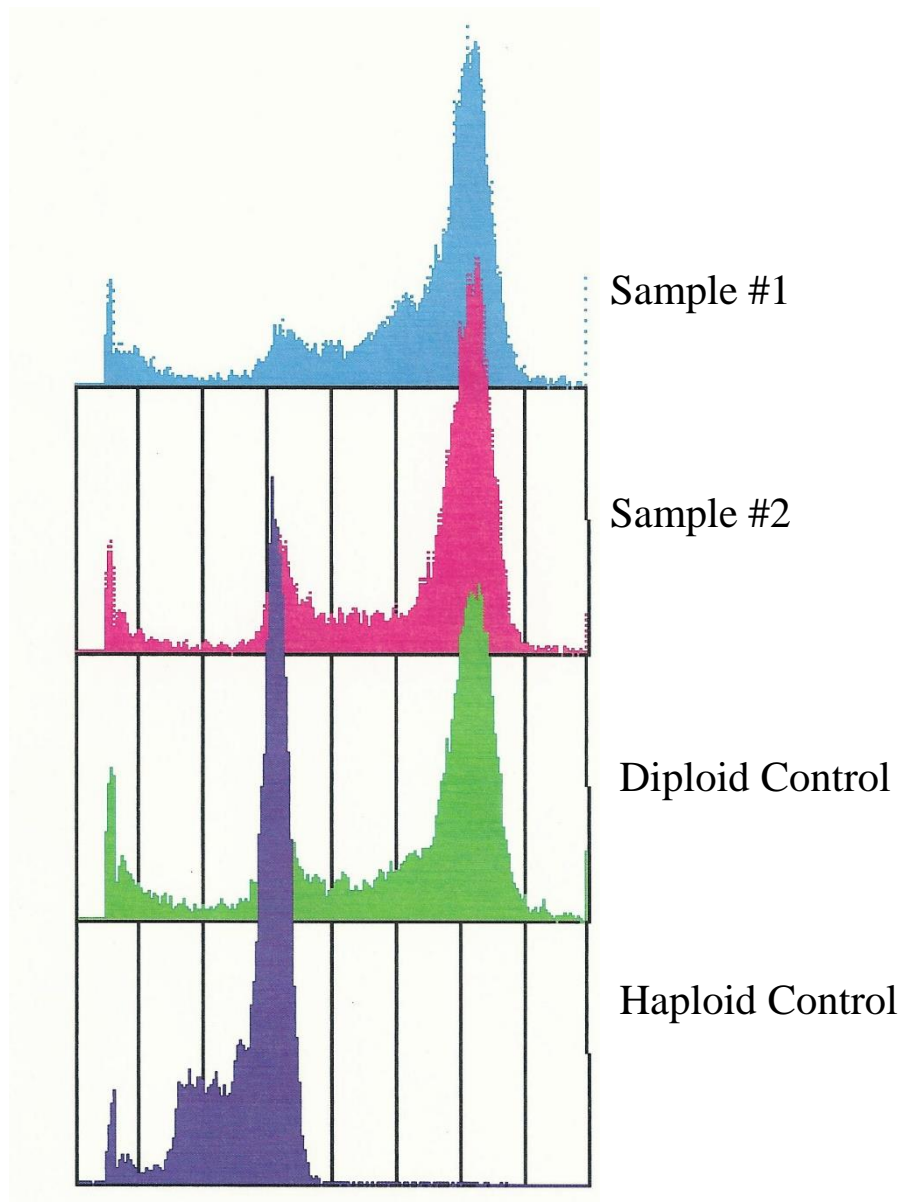
Figure 23: Diploid Confirmation of Replacement of Spo4 by Speroplast FACS

Two colonies from the transformation to replace Spo4 with Ura5 + Lys7 were suggested to be diploid by initial PCR amplification. The result in Figure 22 that the colonies were diploid was confirmed by FACS. The two samples on the top in blue and pink are compared to a diploid control in green and haploid control in purple.
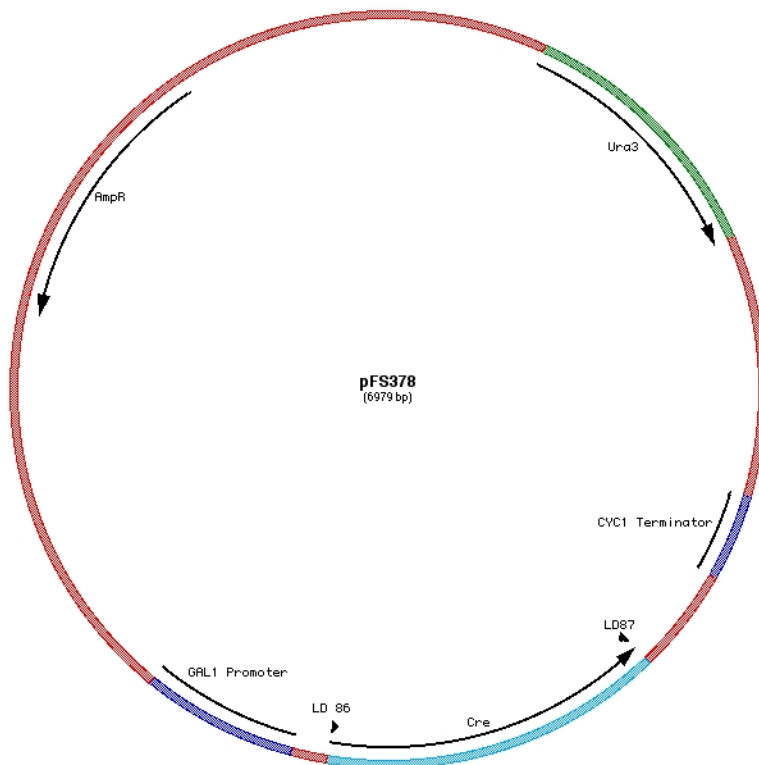
Figure 24: Plasmid Map of pFS378

Gene map of pFS378 used for sense and antisense integration of Cre at Spo6, Spo4, and Mde2 (Figure 12C and 12D) by replacing pFS385 cassette in Figure 12B.

Tables

Table 1: Yeast and Bacterial Strains

Yeast and Bacterial Strains:	
Strains used in Time Courses:	
yFS105	Wild Type (h-)
yFS787	Pac1 - Temperature Sensitive (ts)
yFS118	Pac1-ts; Dcr1Δ
yFS799	Mei4Δ
yFS800	Pac1-ts; Mei4Δ
Strains used for In Vivo Assay	
yFS104	Wild Type (h+)
yFS808	Ura4- Lys-
yLD124	yFS808 with Ura+ Lys+ at Spo6
yLD125	yFS808 with Ura+ Lys+ at Spo4
yLD126	yFS808 with Ura+ Lys+ at Mde2
pFS181	Gibson Assemby Vector
pFS240	Leu2 Cre Expression Plasmid
pFS241	Ura4 Cre Expression Plasmid
pFS385	Lys+ Ura+
pFS378	CRE
pFS387	RFP/GFP Cassette

Table 2: Primers used to Check Integrations

Name	Sequence	Function
LD1	CCAAGAACACCATAAAAACTCTCC	In genomic regoin as PCR control Forward
LD2	CGTTTGCATAGGAGATCCA	In genomic regoin as PCR control Reverse
RH22	TCTTTCCGAGTCAATCCGGA	Inside Coding Region of Spo6
LD101	CAGATCCTTCAGGAATGCGA	Outside Spo6 Forward
LD140	GACGACGTGATTGCTCATCA	Outside Spo6 Reverse
RH36	AATTGGAGTGCTTCATTGGC	Outside Spo4 Forward
RH37	AGATGTTTGCAACGCACGC	Outside Spo4 Reverse
RH09	TGGTGCGTACTTAAGAGACC	Inside Coding Region of Spo4 Forward
RH44	AAGGCATTCGTTCGTGAGT	Outside Mde2 Forward
RH45	AGCTACCTGCTTACCTACAG	Outside Mde2 Reverse
RH11	GATAACTCACATGCATCTCC	Inside Coding Region of Mde2 Forward
LD93	TGTAGAGAAGGCACTTAGCC	Inside Coding region of CRE
RH26	GTACTGAGAGTGCACCATAC	Inside the RFP/GFP cassette upstream of the Leu1 UTR Forward
RH27	ATATGCGCCAGAAATGTACG	Downstream of the genomic Leu1 gene Reverse
RH28	GTTGTTGTTAGGGCATGCAAG	Inside the RFP/GFP cassette downstream of the Leu1 UTR Reverse
RH29	CTGGTCATTTACGTTACTG	Upstream of the genomic Leu1 gene Forward

Table 3: Amplification Primers

Name	Sequence	Function
RH06	GGAACAGGAAATGACAGCATC	RT Ade4 Sense
RH07	CTGGTAGAAGAAGGGAGTTA	RT Spo6 Antisense
RH08	CCATCAACTGCTGATTCTGT	RT Spo6 Sense
LD17	ACCATCCAGCTCACGAAATC	qPCR Spo6 Reverse
LD18	GATTTGACGGCACCAAACAC	qPCR Spo6 Forward
LD9	TCAAATCCTTCCTTGCCTAA	qPCR Ade4 Reverse
LD10	CATGTAATCGGGACCAAACC	qPCR Ade4 Forward
LD99	GGTGAATTCATCAGCCTCCCAAGGAATATATATACACTACTTCTTCCTAAAATCTTCCGGAAGAGT - CTCATTTGGCTTGGTACTGCTG	Unmarked knockout of Spo6 using pFS385 (Hoffman plasmid) Forward
LD100	AGAGTGTATCACCAATGAGCTTCCCACGCTTGGGAAAACCAGTCTAACTTATTTAAATCTATTTGATTTAAACTGATA - ATTACAAGTCGTTCAAATGTCTCCC	Unmarked knockout of Spo6 using pFS385 (Hoffman plasmid) Reverse
LD86	GGTGAATTCATCAGCCTCCCAAGGAATATATATACACTACTTCTTCCTAAAATCTTCCGGAGTCAAATCCGGAAGAGT - ATGTCCAATTACTGACCGT	Ura4 knockout at Spo6 locus w/ Cre cassette - Sense - Forward
LD87	AGAGTGTATCACCAATGAGCTTCCCACGCTTGGGAAAACCAGTCTAACTTATTTAAATCTATTTGATTTAAACTGATA - CTAATCGCCATCTTCCAGCA	Ura4 knockout at Spo6 locus w/ Cre cassette - Sense - Reverse
LD88	GGTGAATTCATCAGCCTCCCAAGGAATATATATACACTACTTCTTCCTAAAATCTTCCGGAAGAGT - CTAATCGCCATCTTCCAGCA	Ura4 knockout at Spo6 locus w/ Cre cassette - Antisense - Forward
LD89	AGAGTGTATCACCAATGAGCTTCCACGCTTGGGAAAACCAGTCTAACTTATTTAAATCTATTTGATTTAAACTGATA - ATGTCCAATTACTGACCGT	Ura4 knockout at Spo6 locus w/ Cre cassette - Antisense - Reverse
RH30	TATTAATGAAAATTGTCCTATCTAACAGCCCGGCACTTTACCAAACAAAAATAAAAATAAAAACAGGAA - CTCATTTGGCTTGGTACTGCTG	Unmarked knockout of Spo4 using pFS385 (Hoffman plasmid) Forward
RH31	TCGATACAATAAAATAAAACTTTGAATGATTATTGGAATTCGGACATACACGT - ATTACAAGTCGTTCAATGTCTCCC	Unmarked knockout of Spo4 using pFS385 (Hoffman plasmid) Reverse
RH32	TATTAATGAAAATTGTCCTATCTAACAGCCCGGCACTTTACCAAACAAAAATAAAAACAGGAA - ATGTCCAATTACTGACCGT	Ura4 knockout at Spo4 locus w/ Cre cassette - Sense - Forward
RH33	TCGATACAATAAAATAAAACTTTGAATGATTATTGGAATTCGGACATACACGT - CTAATCGCCATCTTCCAGCA	Ura4 knockout at Spo4 locus w/ Cre cassette - Sense - Reverse
RH34	TATTAATGAAAATTGTCCTATCTAACAGCCCGGCACTTTACCAAACAAAAATAAAAACAGGAA - CTAATCGCCATCTTCCAGCA	Ura4 knockout at Spo4 locus w/ Cre cassette - Antisense - Forward
RH35	TCGATACAATAAAATAAAACTTTGAATGATTATTGGAATTCGGACATACACGT - ATGTCCAATTACTGACCGT	Ura4 knockout at Spo4 locus w/ Cre cassette - Antisense - Reverse
RH38	ACCATACTACTAAGACAACAACCAAAGTGAATGGGTAATTCAAGACTAAAAGAAGAGGATCACGGAA - CTCATTTGGCTTGGTACTGCTG	Unmarked knockout of Mde2 using pFS385 (Hoffman plasmid) Forward
RH39	TCCAAATATGTAACGATACTCCATCACTTCTTCCTTGACCCAAAACTTGTTAGCTTAAATTCCTTACAAAAAA - ATTACAAGTCGTTCAATGTCTCCC	Unmarked knockout of Mde2 using pFS385 (Hoffman plasmid) Reverse
RH40	ACCATACTACTAAGACAACAACCAAAGTGAATGGGTAATTCAAGACTAAAAGAAGAGGATCACGGAA - ATGTCCAATTACTGACCGT	Ura4 knockout at Mde2 locus w/ Cre cassette - Sense - Forward
RH41	TCCAAATATGTAACGATACTCCATCACTTCTTCCTTGACCCAAAACTTGTTAGCTTAAATTCCTTACAAAAAA - CTAATCGCCATCTTCCAGCA	Ura4 knockout at Mde2 locus w/ Cre cassette - Sense - Reverse
RH42	ACCATACTACTAAGACAACAACCAAAGTGAATGGGTAATTCAAGACTAAAAGAAGAGGATCACGGAA - CTAATCGCCATCTTCCAGCA	Ura4 knockout at Mde2 locus w/ Cre cassette - Antisense - Forward
RH43	TCCAAATATGTAACGATACTCCATCACTTCTTCCTTGACCCAAAACTTGTTAGCTTAAATTCCTTACAAAAAA - ATGTCCAATTACTGACCGT	Ura4 knockout at Mde2 locus w/ Cre cassette - Antisense - Reverse
RH19	TTCCTGCAGGTCGACTCTAGCACCAGAACTTAGTTCGACGG	pFS387 Amplification for Gibson Assembly Forward
RH16	GGGAACAAAAGCTGGAGCTCTGCCGGGTAGAGGTGTGGT	pFS387 Amplification for Gibson Assembly Reverse
RH20	GTCGAAACTAAGTTCTGGTGTGCTAGAGTCGACCTGCAGGA	pFS181 Amplification for Gibson Assembly Forward
RH21	TGACCACACCTCTACCGGCAGAGCTCCAGCTTTTGTTCC	pFS181 Amplification for Gibson Assembly Reverse

Reference

(1-37)

1. (2006) Selective elimination of messenger RNA prevents an incidence of untimely meiosis, *Nature 442*, 45-50.

2. (2009) Regulatory roles of natural antisense transcripts, *Nature Reviews Molecular Cell Biology 10*, 637-643.

3. Bitton, D. A., Miller, C. J., Grallert, A., Scutt, P. J., Yates, T., Li, Y., Bradford, J. R., Hey, Y., Pepper, S. D., and Hagan, I. M. (2011) Programmed fluctuations in sense/antisense transcript ratios drive sexual differentiation in S. pombe, *Molecular systems biology 7*, 559.

4. Carmichael, J. B., Provost, P., Ekwall, K., and Hobman, T. C. (2004) Ago1 and Dcr1, two core components of the RNA interference pathway, functionally diverge from Rdp1 in regulating cell cycle events in Schizosaccharomyces pombe, *Mol. Biol. Cell 15*, 1425-1435.

5. Chen, H.-M., Rosebrock, A. P., Khan, S. R., Futcher, B., and Leatherwood, J. K. (2012) Repression of meiotic genes by antisense transcription and by Fkh2 transcription factor in Schizosaccharomyces pombe, *PloS One 7*, e29917.

6. Dutrow, N., Nix, D. A., Holt, D., Milash, B., Dalley, B., Westbroek, E., Parnell, T. J., and Cairns, B. R. (2008) Dynamic transcriptome of Schizosaccharomyces pombe shown by RNA-DNA hybrid mapping, *Nat. Genet. 40*, 977-986.

7. Gobeil, L.-A., Plante, P., Rohani, M., Ouellette, M., and Provost, P. (2008) Involvement of Dcr1 in post-transcriptional regulation of gene expression in Schizosaccharomyces pombe, *Front. Biosci. 13*, 2203-2215.

8. Gould, K. L., and Simanis, V. (1997) The control of septum formation in fission yeast, *Genes Dev. 11*, 2939-2951.

9. Goyal, A., Takaine, M., Simanis, V., and Nakano, K. (2011) Dividing the spoils of growth and the cell cycle: The fission yeast as a model for the study of cytokinesis, *Cytoskeleton (Hoboken)*.

10. Iino, Y., Sugimoto, A., and Yamamoto, M. (1991) S. pombe pac1+, whose overexpression inhibits sexual development, encodes a ribonuclease III-like RNase, *The EMBO journal 10*, 221-226.

11. Kumar, M., and Carmichael, G. G. (1998) Antisense RNA: function and fate of duplex RNA in cells of higher eukaryotes, *Microbiol Mol Biol Rev 62*, 1415-1434.

12. Lilley, D. M. J., and Sutherland, J. (2011) The chemical origins of life and its early evolution: an introduction, *Philos. Trans. R. Soc., B 366*, 2853-2856.

13. Mata, J., Lyne, R., Burns, G., and Baehler, J. (2002) The transcriptional program of meiosis and sporulation in fission yeast, *Nat. Genet. 32*, 143-147.

14. Mitchison, J. M., and Nurse, P. (1985) Growth in cell length in the fission yeast Schizosaccharomyces pombe, *J Cell Sci 75*, 357-376.

15. Miyawaki, A., Nagai, T., and Mizuno, H. (2003) Mechanisms of protein fluorophore formation and engineering, *Curr. Opin. Chem. Biol. 7*, 557-562.

16. Mudge, D. K., Hoffman, C. A., Lubinski, T. J., and Hoffman, C. S. (2012) Use of a ura5 +-lys7 + cassette to construct unmarked gene knock-ins in Schizosaccharomyces pombe, *Curr. Genet. 58*, 59-64.

17. Nakamura, T., Kishida, M., and Shimoda, C. (2000) The Schizosaccharomyces pombe spo6+ gene encoding a nuclear protein with sequence similarity to budding yeast Dbf4 is required for meiotic second division and sporulation, *Genes Cells 5*, 463-479.

18. Nakamura, T., Nakamura-Kubo, M., Nakamura, T., and Shimoda, C. (2002) Novel fission yeast Cdc7-Dbf4-like kinase complex required for the initiation and progression of meiotic second division, *Mol. Cell. Biol. 22*, 309-320.

19. Ni, T., Tu, K., Wang, Z., Song, S., Wu, H., Xie, B., Scott, K. C., Grewal, S. I., Gao, Y., and Zhu, J. (2010) The prevalence and regulation of antisense transcripts in Schizosaccharomyces pombe, *PLoS One 5*, e15271.

20. Nicholson, A. W. (2001) *Ribonucleases, Part B: Artificial and Engineered Ribonucleases and Speicifc Applications: Artificial and Engineered Ribonucleases and Speicifc Applications*, Elsevier Science.

21. Pyle, A. M. (1993) Ribozymes: a distinct class of metalloenzymes, *Science 261*, 709-714.

22. Rhind, N., Heiman, D. I., Young, S. K., Furuya, K., Guo, Y., Pidoux, A., Robbertse, B., Goldberg, J. M., Aoki, K., Bayne, E. H., Chen, H. M., Chen, Z., Berlin, A. M., Desjardins, C. A., Dobbs, E., Dukaj, L., Fan, L., FitzGerald, M. G., French, C., Gujja, S., Hansen, K., Keifenheim, D., Yassour, M., Levin, H., Levin, J. Z., Mosher, R. A., Müller, C. A., Pfiffner, J., Priest, M., Russ, C., Smialowska, A., Swoboda, P., Sykes, S. M., Vaughn, M., Thompson, D. A., Vengrova, S., Yoder, R., Zeng, Q., Allshire, R., Baulcombe, D., Birren, B. W., Brown, W., Ekwall, K., Kellis, M., Leatherwood, J., Haas, B. J., Margalit, H., Martienssen, R., Nieduszynski, C. A., Spatafora, J. W., Friedman, N., Dalgaard, J. Z., Baumann, P., Niki, H., Regev, A., Habib, N., Nusbaum, C., Wapinski, I., Roy, S., and Lin, M. F. (2011) Comparative Functional Genomics of the Fission Yeasts, *Science 332*, 930-936.

23.   Rotondo, G., and Frendewey, D. (1996) Purification and Characterization of the Pac1 Ribonuclease of Schizosaccharomyces Pombe, *Nucleic Acids Research 24*, 2377-2386.

24.   Rotondo, G., and Frendewey, D. (2001) Pac1 ribonuclease of Schizosaccharomyces pombe, *Methods Enzymol 342*, 168-193.

25.   Rutledge, R. G. (2004) Sigmoidal curve-fitting redefines quantitative real-time PCR with the prospective of developing automated high-throughput applications, *Nucleic Acids Research 32*, e178-e178.

26.   Schmidt, M. W., Houseman, A., Ivanov, A. R., and Wolf, D. A. (2007) Comparative proteomic and transcriptomic profiling of the fission yeast Schizosaccharomyces pombe, *Mol. Syst. Biol.*, No pp. given.

27.   Shendure, J., and Church, G. M. (2002) Computational discovery of sense-antisense transcription in the human and mouse genomes, *GenomeBiology 3*, No pp. given.

28.   Tanabe, K., Ito, N., Wakuri, T., Ozoe, F., Umeda, M., Katayama, S., Tanaka, K., Matsuda, H., and Kawamukai, M. (2003) Sla1, a Schizosaccharomyces pombe homolog of the human La protein, induces ectopic meiosis when its C terminus is truncated, *Eukaryotic Cell 2*, 1274-1287.

29.   Tsien, R. Y. (1998) The green fluorescent protein, *Annu. Rev. Biochem. 67*, 509-544.

30.   Van, D. G. D. (2001) A structural view of cre-loxp site-specific recombination, *Annu Rev Biophys Biomol Struct 30*, 87-104.

31.   van Werven, F. J., Neuert, G., Hendrick, N., Lardenois, A., Buratowski, S., van Oudenaarden, A., Primig, M., and Amon, A. (2012) Transcription of two long non-coding RNAs mediates mating type control of gametogenesis in budding yeast, *Cell 150*, 1170-1181.

32.   Verdel, A., Vavasseur, A., Le, G. M., and Touat-Todeschini, L. (2009) Common themes in siRNA-mediated epigenetic silencing pathways, *Int J Dev Biol 53*, 245-257.

33.   Wall, M. A., Socolich, M., and Ranganathan, R. (2000) The structural basis for red fluorescence in the tetrameric GFP homolog DsRed, *Nat Struct Biol 7*, 1133-1138.

34.   Wilson, J., and Hunt, T. (2002) *Molecular biology of the cell: a problems approach*, Garland Science, New York.

35.   Wood, V., Gwilliam, R., Rajandream, M. A., Lyne, M., Lyne, R., Stewart, A., Sgouros, J., Peat, N., Hayles, J., Baker, S., Basham, D., Bowman, S., Brooks, K., Brown, D., Brown, S., Chillingworth, T., Churcher, C., Collins, M., Connor, R., Cronin, A., Davis, P., Feltwell, T., Fraser, A., Gentles, S., Goble, A., Hamlin, N., Harris, D., Hidalgo, J., Hodgson, G., Holroyd, S., Hornsby, T., Howarth, S., Huckle, E. J., Hunt, S., Jagels, K.,

James, K., Jones, L., Jones, M., Leather, S., McDonald, S., McLean, J., Mooney, P., Moule, S., Mungall, K., Murphy, L., Niblett, D., Odell, C., Oliver, K., O'Neil, S., Pearson, D., Quail, M. A., Rabbinowitsch, E., Rutherford, K., Rutter, S., Saunders, D., Seeger, K., Sharp, S., Skelton, J., Simmonds, M., Squares, R., Squares, S., Stevens, K., Taylor, K., Taylor, R. G., Tivey, A., Walsh, S., Warren, T., Whitehead, S., Woodward, J., Volckaert, G., Aert, R., Robben, J., Grymonprez, B., Weltjens, I., Vanstreels, E., Rieger, M., Schaefer, M., Mueller-Auer, S., Gabel, C., Fuchs, M., Duesterhoeft, A., Fritzc, C., Holzer, E., Moestl, D., Hilbert, H., Borzym, K., Langer, I., Beck, A., Lehrach, H., Reinhardt, R., Pohl, T. M., Eger, P., Zimmermann, W., Wedler, H., Wambutt, R., Purnelle, B., Goffeau, A., Cadieu, E., Dreano, S., Gloux, S., Lelaure, V., Mottier, S., Galibert, F., Aves, S. J., Xiang, Z., Hunt, C., Moore, K., Hurst, S. M., Lucas, M., Rochet, M., Gaillardin, C., Tallada, V. A., Garzon, A., Thode, G., Daga, R. R., Cruzado, L., Jimenez, J., Sanchez, M., del, R. F., Benito, J., Dominguez, A., Revuelta, J. L., Moreno, S., Armstrong, J., Forsburg, S. L., Cerutti, L., Lowe, T., McCombie, W. R., Paulsen, I., Potashkin, J., Shpakovski, G. V., Ussery, D., Barrell, B. G., and Nurse, P. (2003) The genome sequence of Schizosaccharomyces pombe, *Nature (London, U. K.) 421*, 94.

36.   Yanagida, M. (2002) The model unicellular eukaryote, Schizosaccharomyces pombe, *GenomeBiology 3*, No pp. given.

37.   Yang, F., Moss, L. G., and Phillips, G. N., Jr. (1996) The molecular structure of green fluorescent protein, *Nat. Biotechnol. 14*, 1246-1251.